Pediatric RESEARCH

Diffuse Optical Tomography to Investigate the Newborn Brain

Journal:	*Pediatric Research*
Manuscript ID	PR-2016-0467.R2
Manuscript Type:	Review article
Date Submitted by the Author:	n/a
Complete List of Authors:	Lee, Chuen Wai; neoLAB, The Evelyn Perinatal Imaging Centre; Cambridge University Hospitals NHS Foundation Trust, Department of Neonatology Cooper, Robert; neoLAB, The Evelyn Perinatal Imaging Centre; University College London, Department of Medical Physics and Biomedical Engineering Austin, Topun; neoLAB, The Evelyn Perinatal Imaging Centre; Cambridge University Hospitals NHS Foundation Trust, Department of Neonatology
Keywords:	Infant, Near-Infrared Spectroscopy, Optical Imaging

Diffuse Optical Tomography to Investigate the Newborn Brain

Chuen Wai Lee[1,2], Robert J Cooper[1,3], Topun Austin[1,2]

1. neoLAB, The Evelyn Perinatal Imaging Centre, The Rosie Hospital, Cambridge University Hospitals NHS Foundation Trust, Cambridge, United Kingdom, 2. Department of Neonatology, The Rosie Hospital, Cambridge University Hospitals NHS Foundation Trust, Cambridge, United Kingdom, 3. Department of Medical Physics and Biomedical Engineering, University College London, London, United Kingdom.

Running Title

Diffuse Optical Tomography in Newborns

Corresponding author

Topun Austin Email: topun.austin@addenbrookes.nhs.uk

Department of Neonatology, The Rosie Hospital, Cambridge University Hospitals NHS Foundation Trust, Cambridge Biomedical Campus, Hills Road, Cambridge, CB2 0QQ, UK

Tel: 01223 256947

Conflict of Interest Statement

The authors have no conflicts of interest relevant to this article to disclose.

Funding

This work was supported by the Medical Research Council, London UK (MR/L017490/1), the Evelyn Trust, Cambridge UK (09/26 2013 RTF) and the Engineering and Physical Sciences Research Council, London UK (EP/N025946/1).

Word Count

Manuscript: 4602 words

Abstract: 134 words

Abstract

Over the past 15 years, functional near-infrared spectroscopy (fNIRS) has emerged as a powerful technology for studying the developing brain. Diffuse Optical Tomography (DOT) is an extension of fNIRS that combines hemodynamic information from dense optical sensor arrays over a wide field of view. Using image reconstruction techniques, DOT can provide images of the hemodynamic correlates to neural function that are comparable to those produced by functional MRI (fMRI).

This review article explains the principles of DOT, and highlights the growing literature on the use of DOT in the study of healthy development of the infant brain, and the study of novel pathophysiology in infants with brain injury. Current challenges, particularly around instrumentation and image reconstruction, will be discussed as will the future of this growing field, with particular focus on whole-brain, time-resolved DOT.

Introduction

The field of medical physics and biomedical engineering has provided a range of novel neuroimaging techniques that have enabled scientists and clinicians to investigate the functional organization and architecture of the human brain in health and disease. In recent years, functional near-infrared spectroscopy (fNIRS) has become an increasingly valuable tool. As well as being non-invasive, relatively low-cost and easy to set up, it can be carried out in infants who are awake and do not need to be transported to specialized imaging facilities. Diffuse optical tomography (DOT) is a natural extension of fNIRS, which combines multichannel data acquisition with image reconstruction software to provide images of changes in regional blood volume and oxygenation at high temporal and spatial resolution. This technology is increasingly being used by researchers and clinicians to study healthy brain development as well as pathophysiology in critically ill infants in intensive care. Figure 1 summarizes the terminology and NIRS domains that will be described in this paper.

The aim of this paper is to explain the principles of DOT and highlight studies using DOT in newborn infants. We also summarize the current challenges of the technique and discuss the future of the field, with particular emphasis on technological developments and time-domain DOT techniques.

Principles of Optical Imaging

Near-Infrared Spectroscopy (NIRS)

Near-infrared spectroscopy (NIRS) is a non-invasive tissue monitoring technique that exploits the relative transparency of biological tissue to near-infrared light (650-950nm) and

the wavelength dependent absorption characteristics of light absorbing compounds, or chromophores. In the brain, haemoglobin is the dominant chromophore, whose absorption varies with oxygenation, first described by Jöbsis in 1977 (1-3) (Figure 2a).

However, the dominant interaction between near-infrared light and tissue is not absorption but scattering, such that the path travelled by a given photon will constitute a 'random walk': bouncing randomly from one scattering event to the next. Near-infrared light therefore forms a *diffuse* field when entering tissue. Assuming scattering remains constant, loss of light, or attenuation, will be due to changes in absorption by the main chromophores (light absorbing molecules). The simplest form of NIRS measurement consists of two wavelengths of NIR light, coupled into tissue via an optical fiber positioned a few centimetres away to collect light and transmit it to a detector. This method has been used extensively to study cerebral oxygenation in the newborn infant (4, 5) (for a review see (6)).

Functional Near-Infrared Spectroscopy (fNIRS)

During cortical activation, neural excitation produces an increased metabolic demand that results in local changes in oxygen consumption, vasodilatation, increased blood flow and increased oxygenation. This relationship, between neural activity and vasodilation, is known as neurovascular coupling. In adults, a local increase in neural activity is typically characterized by an increase in oxyhemoglobin concentration and a decrease in deoxyhemoglobin concentration, due to the rapid influx of oxygenated blood (7, 8). While the exact mechanisms of neurovascular coupling are still a matter of active investigation, the consistency of the functional hemodynamic response means that it provides an effective indirect measure of cortical function. As NIRS is able to monitor changes in the concentration of oxy- and deoxy-hemoglobin, the technique can be used to measure the functional hemodynamic response to specific stimuli. This technique is known as functional

NIRS or fNIRS. The same physiological principles exploited by fNIRS underpin the blood oxygen level dependent (BOLD) signal, which is used in functional MRI (fMRI). However, while the BOLD signal is predominantly sensitive to the concentration of deoxyhemoglobin (9), fNIRS methods have the advantage of being able to monitor the concentrations of both oxy- and deoxy-hemoglobin independently, which significantly aids the physiological interpretation of fNIRS measurements.

In infants, the maturity of neurovascular coupling is still in question, and studies have yielded adult-like responses (10-12), inverted (decreased oxyhaemoglobin and increased deoxyhaemoglobin) responses (13) or a mixture of the two (14, 15). Although the nature of this response remains controversial (and is beyond the scope of this review), hemodynamic changes that are temporally correlated to the external stimulus can still provide an indication of neural activation, and the interpretation of response polarity should be carefully assessed depending on the nature of the subject or study.

Early Application of fNIRS in Infants

Early infant functional studies typically used a single source and detector providing one channel i.e. one measurement of the cortical changes in a primary area of interest (14, 16, 17). However, the majority of commercial fNIRS systems now employ numerous source and detector fibers into an array that provides multiple fNIRS channels facilitating the examination of extended cortical regions. The most widely used multi-channel systems are continuous wave (CW) devices, which are relatively low cost and simple to set up (for review of CW systems see (18)).

Multi-channel CW systems measure light attenuation by continuous illumination of the head with multiple sources. To distinguish which source gave rise to the light measured at any given detector, either time or frequency multiplexing methods must be used. In time multiplexing, each source is illuminated in turn for a specific period of time, so that the origin of any detected light is always apparent. In frequency multiplexing, all the sources are illuminated continuously, but with each source modulated at a distinct frequency. CW systems typically allow a sampling rate from 5 to 100 Hz, providing accurate temporal information on cortical hemodynamic activity (19).

Two-Dimensional Mapping and Optical Topography

The simplest approach to obtaining images of spatial variation of brain activity using near-infrared methods is to create a two-dimensional map of the responses obtained using multi-channel CW fNIRS devices. These two-dimensional representations can be generated by interpolating the signal measured by multiple fNIRS channels across the interrogated area (20, 21). This approach is often referred to as optical topography. While this technique has helped accelerate our understanding of neurodevelopment and cognition in the infant brain, including language (22-25), vocal (26, 27), social (28) and face (29) perception (for more reviews (30-33)), the anatomical registration and spatial resolution of the resulting images is limited, and the quantitative accuracy of the images can be compromised (34). It is important to note, however, that significant functional information can be obtained without absolute quantification; fMRI is rightly considered the gold-standard in functional neuroimaging, but in most common applications it remains purely qualitative (35).

Diffuse Optical Tomography

Diffuse optical tomography (DOT) enables the production of three-dimensional images. The term "diffuse" describes the path of near-infrared light when it enters tissue (as explained in the "Principles of Optical Imaging" section). Unlike 2D topographic approaches, DOT exploits measurements from multiple overlapping channels, with a range of source-detector distances to obtain depth information. A major advantage of this approach is the ability to separate hemodynamics occurring at different depths, and thus reduce the influence of blood oxygenation changes in extracerebral tissues such as the scalp or skull (see section titled "Physiological signal contamination").

The quality of DOT images is dependent on the number of channels that sample a given volume of tissue. The total number of channels one can achieve is dependent on the size and weight of the optical fibers and the number of source and detectors available in a DOT system. While a sparse array can provide whole-head coverage (36), the resulting spatial resolution can be compromised. At present, commercial devices that can perform DOT (Figure 2c) provide 10-20 sources and 10-20 detectors, which allow imaging of sub-sections of the adult cortex, or the majority of the infant cortex. Image resolution is a function of array density, such that dense arrays provide better spatial resolution (37). However, no DOT system (commercially available or otherwise) has yet been demonstrated that can provide dense sampling (i.e. with a nearest-neighbor source detector separation of < 15 mm) over the whole scalp of either the infant or the adult (38).

DOT Image Reconstruction

DOT image reconstruction is an example of an inverse problem, in which the goal is to determine internal features of an object using measurements of light transmitted between points on the surface. DOT image reconstruction is ill-posed and highly under-determined.

Ill-posed, meaning that many different internal configurations could equally explain the measurements made at the surface (i.e. there is not a unique solution) and highly underdetermined, meaning that the number of unknowns (i.e. voxels in our image) far exceeds the number of measurements made at the surface. One approach to simplify this problem is to produce images of a difference between two points in time, rather than to attempt to create images of the absolute optical properties of the brain. By assuming the changes that have occurred between these two time points are small relative to the background optical characteristics of the tissue, the DOT reconstruction problem can be linearized, significantly simplifying the mathematical challenge (39). A schematic of DOT image reconstruction is shown in Figure 3 and for a more complete summary see (39-41).

Application of DOT in the Newborn Brain

The earliest infant DOT images were reconstructed in the late 1990s. For example, hemodynamic changes over the sensorimotor regions were demonstrated in the premature infant cortex by Chance et al. (42) using a system consisting of nine sources and four detectors. Hintz et al. (13) reconstructed functional images of passive arm movements over the motor cortex in preterm infants using an array with 9 sources and 16 detectors providing 144 independent measurements or channels.

More recently the neonatal application of DOT become more widespread. In a study of healthy newborn infants, Liao et al. used a CW high-density DOT system to image functional activation of the primary visual cortex (43). To counteract the effect of superficial haemodynamic signals from the extra-cerebral tissue, superficial signal regression between the first- and second-nearest source detector paired channels was carried out. Bilateral

increases in oxyhemoglobin concentration were apparent in response to visual stimuli in the reconstructed DOT images. A direct comparison of the hemodynamic response in the DOT images was carried out with the conventionally recorded hemodynamic changes in the source-detector channels. This demonstrated an increase in the signal-to-noise ratio of the DOT images by two-fold compared to the channel-wise data.

Intrinsic brain activity at rest in the absence of a stimulus can also provide information on functional cerebral development. This field, originally established using the BOLD signal in fMRI research, is known as resting state functional connectivity (RSFC) (44) and RSFC networks characterized by bilateral cortical connectivity have been described in the term and preterm infant (45-48).

Focusing on the visual cortex, White et al. produced the first DOT images of bilateral occipital connectivity at rest in preterm and full-term born infants (49). An array consisting of 18 sources and 16 detectors was placed over the occipital cortex to record resting-state brain activity for up to 20 minutes. To identify connectivity, two standard approaches: seed-based analysis and independent component analysis (ICA) were carried out on the DOT images. Visual networks with bilateral connectivity between both cerebral hemispheres in the visual cortex were identified in the full-term and healthy preterm groups. Interestingly, one preterm subject with a diagnosis of a left occipital infarct displayed unilateral connectivity only demonstrating the sensitivity of DOT to cerebral pathology.

In a recent study, Ferradal et al. also identified bilateral cortical connectivity in the resting-state in healthy full-term born infants using both fMRI and DOT imaging modalities in the same subjects for the first time (38). DOT resting-state data were recorded for up to 60

minutes using a dense array of 32 sources and 34 detectors over the temporal and occipital cortices. MRI scans were performed within a day following DOT scanning and subject-specific structural MRI head models of light propagation were used. Using seed-based analysis and ICA, the DOT images revealed bilateral connectivity in the visual, middle temporal and primary auditory networks. Comparisons between the DOT and fMRI seed based maps confirmed strong qualitative and quantitative agreement (Figure 4).

Application of DOT to Investigate Infant Pathology

Perinatal hypoxic ischemic encephalopathy (HIE) is a major cause of mortality and neurodevelopmental disability in term infants (50) resulting from severe perinatal deficit in cerebral blood flow and oxygen delivery (51). Subsequent brain injury is clinically characterized by seizure activity and abnormal neurological function, which may be associated with hemodynamic changes. DOT can offer valuable information on cerebral hemodynamics and oxygenation associated with brain injury, which are currently not available in the clinical setting. In a simultaneous EEG and DOT study of neurologically compromised infants, large transient hemodynamic events were identified in a small group of newborn infants diagnosed with clinical symptoms of seizures (52). Hemodynamic events were characterized by a slow increase in oxyhemoglobin followed by a rapid decrease before a slow return to baseline (Figure 5).

In a case study using EEG and DOT, Singh et al. reported the first DOT images of hemodynamic responses to electrographic seizures in an infant with severe HIE (36). A flexible head cap with 11 EEG electrodes, and 16 sources and 16 detectors was used to record 60-minutes of data that contained 7 electrographic seizure events lasting 30 – 90 s. Although there was spatial variation, the DOT images revealed an initial small increase in cortical

blood volume followed by a profound and extended decrease lasting several minutes (Figure 6).

In the absence of electrographic seizures, HIE infants may experience electrographic burst suppression which is associated with poor neurodevelopmental prognosis (53). These patterns present as low-voltage electrical activity alternating with sharp high-voltage bursts that occur globally or in focal cortical regions (54). Neuroimaging strategies with improved spatial specificity compared to EEG can provide close monitoring of this pathological state. Using the same flexible DOT-EEG cap array (36), Chalia et al. identified hemodynamic responses relating to electrographic burst events of 4-6 s, in 6 infants with HIE (55). The DOT images demonstrated a decrease in oxyhemoglobin prior to, or during burst activity, followed by a large increase and a return to baseline with an undershoot. Patient-specific spatial patterns that were not apparent in the EEG were observed in the DOT images signifying the complex morphology of burst suppression.

Time-domain DOT

In addition to CW devices which measure only the changes in intensity of the detected light, and are thus unable to separate the effects of absorption and scatter or provide absolute quantification of tissue parameters, researchers have developed what are known as time-resolved or time-domain DOT devices (TD-DOT). TD devices operate by injecting very short pulses of light (picoseconds) in to tissue and measuring the time-of-flight of individual photons using highly sensitive, photon-counting detectors (for review of TD methods, see (56)). By building up a histogram of photon flight-times, TD-DOT provides a rich data set that contains information related to both the absorption and scattering properties of the

underlying tissue. As a result, TD-DOT requires fewer assumptions to be made than CW methods, and it is possible to obtain absolute measurements of oxy- and deoxy-hemoglobin concentrations.

Because TD-DOT employs sensitive photon-counting detectors, it is also possible to make measurements over much larger source-detector distances including across the whole newborn infant head, allowing the creation of DOT images of the entire volume of the infant brain. Early images reconstructed using this technique were able to identify intracranial hemorrhages in preterm infants (57-59) (for an example see Figure 7). Compared with established imaging techniques such as ultrasound, blinded comparisons of DOT images in infants of varying gestation were interpreted as correct in six out of eight cases using TD-DOT (60). Hemodynamic changes induced by adjusting mechanical ventilator settings in a full-term infant with HIE (61) have also been imaged across the whole brain, as have functional hemodynamic changes in the somato-motor cortex during passive arm movement in healthy preterm infants (62).

Continuing Challenges of DOT

Recent advances in DOT have allowed the technique to become an effective method for the investigation of both healthy and pathological neurodevelopment. However, as with all emerging technologies, a number of significant challenges still remain.

Head-gear Array Design

Due to the physical size and weight of optical fibers, and the number of optodes available in a DOT system, the maximum number that can be used is currently limited, particularly for small infants. As a result, investigators employing DOT must still choose between a sparse

whole-head array (36) or a high-density localized array (38). The ability to flexibly design an array to suit a given experiment can be extremely beneficial, but the lack of a single 'catch-all' array solution does make it harder to perform quantitative cross-study comparisons and also hinders the standardization and automation of data processing methods.

Movement Artifacts

Movement can be a significant problem in DOT studies, particularly in awake infants. Relative motion between the optical fibre and the scalp of the subject will affect optical coupling, which will often cause large variations in the measured optical intensity. Typically, the impact of movement on DOT data is to invoke transient, high-amplitude spikes in intensity, which immediately subside when the movement ends. Because these artifacts are temporary, periods of good-quality data DOT can usually be extracted, even in studies of awake infants. Unlike with fMRI, it is therefore rare that a whole DOT data set will have to be discarded due to movement artifacts. There are three broad strategies that can be employed to address the problem of motion in DOT. The first is to prevent motion artifacts from occurring at all; by encouraging the infant to sleep, for example by feeding and swaddling the infant; by ensuring that there are appropriate stimuli to engage an awake infant; and to construct the optode array headgear to optimize the coupling of the optodes to the head. The second is to exclude data that is deemed (by visual inspection or via the use of an accelerometer or video recording) to be contaminated by motion artifact and the third is to use post-processing methods to clean the data to remove the effects of motion (63). In practice, most DOT studies employ all three of these approaches, while NIRS and DOT motion artifact filtering methodologies continue to advance (64, 65).

Physiological signal contamination

One technical limitation common to all forms of NIRS and DOT is contamination of the measured signal by non-neuronal sources. These include systemic hemodynamic changes in both the brain and the superficial layers of the head including the skin caused by the cardiac cycle, blood pressure and respiration. Because of the ability of DOT to obtain 3D information, DOT image reconstruction can inherently separate the scalp and brain layers. Simple approaches employed in NIRS can also be used for DOT, including low-pass filtering of the signal and block averaging to extract the signal that is temporally correlated to an external functional stimulus (18). More recent multivariate techniques, such as superficial signal regression (66-68), which uses short source-detector channels to measure scalp signal, and independent component analysis (ICA) (69, 70) or principal component analysis (PCA) (71-73), have been developed to isolate cerebral signals.

Structural Priors

A major advantage of DOT in comparison to fMRI is its portability. However accurate DOT image reconstruction requires high-quality structural models of the subject's head to act as a prior for image reconstruction. Significant efforts have therefore been made to optimize an age-matched 4D neonatal head model (74) using MRI head atlases as an alternative to subject-specific data (36, 49, 55). An advantage of using a standard atlas is that it facilitates group comparisons across subjects, as it defines a common coordinate space (75) although this reduces the spatial specificity of the DOT images (76). Careful application of the optode array, and measurement of its position relative to certain cranial landmarks using a 3D digitizer can minimize the errors associated with registration and positioning and yield high-quality, anatomically registered DOT images.

Statistical Analysis

As an emerging field, there is as yet no gold-standard approach for determining statistical significance or inference from DOT images (for general review see (77)). To extract the functional response to certain stimuli, event related designs have used a general linear model (GLM) approach to model the hemodynamic changes as a linear combination of independent variables (78). Similar to fMRI analysis, statistical parametric mapping (SPM) tools that use a GLM approach have also been developed and implemented for the statistical analysis of topographic (79) and tomographic images (80). However, there remain some concerns regarding the application of fMRI data processing methodologies to DOT because of the fundamentally different noise characteristics of the two data-types (81). A major bottle-neck in achieving a standardized (or even automated) DOT image reconstruction and processing pipeline is the lack of a 'catch-all' high-density, whole-scalp imaging array.

Future Directions

One of the major confounding limitations of DOT methods remains the necessity of using large numbers of optical fibers. However, technology is rapidly developing that will allow DOT imaging without the use of optical fibres. Lightweight electronics can be worn by a subject with fewer cables in recent 'wearable' fNIRS systems enabling researchers to study mobile adult subjects (19, 82, 83). Chitnis et al. (82) published the first functional images of the human brain obtained with a fibreless, high-density DOT system. Though designed for adults, this technology will likely be adapted for studies of the infant brain. By dispensing with the optical fibers, it may soon be possible to produce a wearable, high-density, whole-scalp DOT system that will provide high-quality functional images of the infant brain continuously at the bedside.

This has significant implications for both developmental neuroscience and clinical practice. For example, this would allow continuous monitoring of resting state cortical connectivity in premature infants as a measurement of cognitive development or the detection of pathological cortical regions such as in stroke.

While these wearable technologies are impressive, they are still CW devices, and thus provide limited quantitation. Historically, TD systems have been large and extremely expensive because of the complex electronics required for photon-counting. The advent of low-cost, solid-state single photon avalanche detectors (SPADs), which are now being developed for a range of novel time-of-flight technologies, will allow the issues of size and cost to be minimized in future generations of instruments (56). It is now reasonable to predict that fibreless TD-DOT technologies that provide quantitative, depth-sensitive, 3D images of the whole infant brain with a resolution of ~5 mm will be available within the next decade.

Conclusions

From the early measurements of cerebral oxygenation in newborns, to the more complex images of functional brain activity in recent years, DOT is rapidly emerging as an important tool for clinicians and neuroscientists to investigate the newborn brain. As the field has grown, so too has the expectation of the technology, and new challenges have arisen as we continue to push the boundaries of DOT. Wearable technologies are now emerging, which have the potential to allow continuous imaging of infant brain function at the cot-side within the next few years. Innovations in TD-DOT technology imply that clinical TD-DOT systems are now on the horizon. As the technology advances, we must ensure that DOT is given the opportunity to become a clinically useful methodology; one that will provide

clinicians with continuous measures of cerebral oxygenation, brain function and neurodevelopment that will complement neonatal intensive care.

References

1. Jöbsis FF 1977 Noninvasive, infrared monitoring of cerebral and myocardial oxygen sufficiency and circulatory parameters. Science 198:1264-1267.
2. van der Zee P, Cope M, Arridge SR, Essenpreis M, Potter LA, Edwards AD, Wyatt JS, McCormick DC, Roth SC, Reynolds EO 1992 Experimentally measured optical pathlengths for the adult head, calf and forearm and the head of the newborn infant as a function of inter optode spacing. Adv Exp Med Biol 316:143-153.
3. Matcher SJ, Cope M, Delpy DT 1994 Use of the water absorption spectrum to quantify tissue chromophore concentration changes in near-infrared spectroscopy. Phys Med Biol 39:177-196.
4. Brazy JE, Lewis DV, Mitnick MH, Jöbsis vander Vliet FF 1985 Noninvasive monitoring of cerebral oxygenation in preterm infants: preliminary observations. Pediatrics 75:217-225.
5. Wyatt JS, Cope M, Delpy DT, Wray S, Reynolds EO 1986 Quantification of cerebral oxygenation and haemodynamics in sick newborn infants by near infrared spectrophotometry. Lancet 2:1063-1066.
6. Wolf M, Greisen G 2009 Advances in near-infrared spectroscopy to study the brain of the preterm and term neonate. Clin Perinatol 36:807-834, vi.
7. Obrig H, Villringer A 2003 Beyond the visible--imaging the human brain with light. J Cereb Blood Flow Metab 23:1-18.
8. Raichle ME, Mintun MA 2006 Brain work and brain imaging. Annu Rev Neurosci 29:449-476.
9. Ogawa S, Lee TM, Kay AR, Tank DW 1990 Brain magnetic resonance imaging with contrast dependent on blood oxygenation. Proc Natl Acad Sci U S A 87:9868-9872.

10. Peña M, Maki A, Kovacić D, Dehaene-Lambertz G, Koizumi H, Bouquet F, Mehler J 2003 Sounds and silence: an optical topography study of language recognition at birth. Proc Natl Acad Sci U S A 100:11702-11705.

11. Taga G, Asakawa K, Maki A, Konishi Y, Koizumi H 2003 Brain imaging in awake infants by near-infrared optical topography. Proc Natl Acad Sci U S A 100:10722-10727.

12. Liao SM, Gregg NM, White BR, Zeff BW, Bjerkaas KA, Inder TE, Culver JP 2010 Neonatal hemodynamic response to visual cortex activity: high-density near-infrared spectroscopy study. J Biomed Opt 15:026010.

13. Hintz SR, Benaron DA, Siegel AM, Zourabian A, Stevenson DK, Boas DA 2001 Bedside functional imaging of the premature infant brain during passive motor activation. J Perinat Med 29:335-343.

14. Meek JH, Firbank M, Elwell CE, Atkinson J, Braddick O, Wyatt JS 1998 Regional hemodynamic responses to visual stimulation in awake infants. Pediatr Res 43:840-843.

15. Kotilahti K, Nissilä I, Näsi T, Lipiäinen L, Noponen T, Meriläinen P, Huotilainen M, Fellman V 2010 Hemodynamic responses to speech and music in newborn infants. Hum Brain Mapp 31:595-603.

16. Bartocci M, Winberg J, Ruggiero C, Bergqvist LL, Serra G, Lagercrantz H 2000 Activation of olfactory cortex in newborn infants after odor stimulation: a functional near-infrared spectroscopy study. Pediatr Res 48:18-23.

17. Zaramella P, Freato F, Amigoni A, Salvadori S, Marangoni P, Suppiej A, Suppjei A, Schiavo B, Chiandetti L 2001 Brain auditory activation measured by near-infrared spectroscopy (NIRS) in neonates. Pediatr Res 49:213-219.

18. Scholkmann F, Kleiser S, Metz AJ, Zimmermann R, Mata Pavia J, Wolf U, Wolf M 2014 A review on continuous wave functional near-infrared spectroscopy and imaging instrumentation and methodology. Neuroimage 85 Pt 1:6-27.

19. Ferrari M, Quaresima V 2012 A brief review on the history of human functional near-infrared spectroscopy (fNIRS) development and fields of application. Neuroimage 63:921-935.

20. Maki A, Yamashita Y, Ito Y, Watanabe E, Mayanagi Y, Koizumi H 1995 Spatial and temporal analysis of human motor activity using noninvasive NIR topography. Med Phys 22:1997-2005.

21. Franceschini MA, Toronov V, Filiaci M, Gratton E, Fantini S 2000 On-line optical imaging of the human brain with 160-ms temporal resolution. Opt Express 6:49-57.

22. Sato H, Hirabayashi Y, Tsubokura H, Kanai M, Ashida T, Konishi I, Uchida-Ota M, Konishi Y, Maki A 2012 Cerebral hemodynamics in newborn infants exposed to speech sounds: a whole-head optical topography study. Hum Brain Mapp 33:2092-2103.

23. Minagawa-Kawai Y, van der Lely H, Ramus F, Sato Y, Mazuka R, Dupoux E 2011 Optical brain imaging reveals general auditory and language-specific processing in early infant development. Cereb Cortex 21:254-261.

24. Homae F, Watanabe H, Nakano T, Taga G 2011 Large-scale brain networks underlying language acquisition in early infancy. Front Psychol 2:93.

25. Gervain J, Macagno F, Cogoi S, Peña M, Mehler J 2008 The neonate brain detects speech structure. Proc Natl Acad Sci U S A 105:14222-14227.

26. Lloyd-Fox S, Blasi A, Mercure E, Elwell CE, Johnson MH 2011 The emergence of cerebral specialization for the human voice over the first months of life. Soc Neurosci.

27. Grossmann T, Oberecker R, Koch SP, Friederici AD 2010 The developmental origins of voice processing in the human brain. Neuron 65:852-858.

28. Lloyd-Fox S, Blasi A, Volein A, Everdell N, Elwell CE, Johnson MH 2009 Social perception in infancy: a near infrared spectroscopy study. Child Dev 80:986-999.

29. Blasi A, Fox S, Everdell N, Volein A, Tucker L, Csibra G, Gibson AP, Hebden JC, Johnson MH, Elwell CE 2007 Investigation of depth dependent changes in cerebral haemodynamics during face perception in infants. Phys Med Biol 52:6849-6864.

30. Lloyd-Fox S, Blasi A, Elwell CE 2010 Illuminating the developing brain: the past, present and future of functional near infrared spectroscopy. Neurosci Biobehav Rev 34:269-284.

31. Gervain J, Mehler J, Werker JF, Nelson CA, Csibra G, Lloyd-Fox S, Shukla M, Aslin RN 2011 Near-infrared spectroscopy: a report from the McDonnell infant methodology consortium. Dev Cogn Neurosci 1:22-46.

32. Aslin RN, Shukla M, Emberson LL 2015 Hemodynamic correlates of cognition in human infants. Annu Rev Psychol 66:349-379.

33. Vanderwert RE, Nelson CA 2014 The use of near-infrared spectroscopy in the study of typical and atypical development. Neuroimage 85 Pt 1:264-271.

34. Boas DA, Dale AM, Franceschini MA 2004 Diffuse optical imaging of brain activation: approaches to optimizing image sensitivity, resolution, and accuracy. Neuroimage 23 Suppl 1:S275-288.

35. Hoge RD 2012 Calibrated FMRI. Neuroimage 62:930-937.

36. Singh H, Cooper RJ, Wai Lee C, Dempsey L, Edwards A, Brigadoi S, Airantzis D, Everdell N, Michell A, Holder D, Hebden JC, Austin T 2014 Mapping cortical haemodynamics during neonatal seizures using diffuse optical tomography: A case study. Neuroimage Clin 5:256-265.

37. Eggebrecht AT, Ferradal SL, Robichaux-Viehoever A, Hassanpour MS, Dehghani H, Snyder AZ, Hershey T, Culver JP 2014 Mapping distributed brain function and networks with diffuse optical tomography. Nat Photonics 8:448-454.

38. Ferradal SL, Liao SM, Eggebrecht AT, Shimony JS, Inder TE, Culver JP, Smyser CD 2016 Functional Imaging of the Developing Brain at the Bedside Using Diffuse Optical Tomography. Cereb Cortex 26:1558-1568.

39. Arridge SR 2011 Methods in diffuse optical imaging. Philos Trans A Math Phys Eng Sci 369:4558-4576.

40. Hoshi Y, Yamada Y 2016 Overview of diffuse optical tomography and its clinical applications. J Biomed Opt 21:091312.

41. Hielscher AH, Bluestone AY, Abdoulaev GS, Klose AD, Lasker J, Stewart M, Netz U, Beuthan J 2002 Near-infrared diffuse optical tomography. Dis Markers 18:313-337.

42. Chance B, Anday E, Nioka S, Zhou S, Hong L, Worden K, Li C, Murray T, Ovetsky Y, Pidikiti D, Thomas R 1998 A novel method for fast imaging of brain function, non-invasively, with light. Opt Express 2:411-423.

43. Liao SM, Ferradal SL, White BR, Gregg N, Inder TE, Culver JP 2012 High-density diffuse optical tomography of term infant visual cortex in the nursery. J Biomed Opt 17:081414.

44. Biswal BB, Van Kylen J, Hyde JS 1997 Simultaneous assessment of flow and BOLD signals in resting-state functional connectivity maps. NMR Biomed 10:165-170.

45. Doria V, Beckmann CF, Arichi T, Merchant N, Groppo M, Turkheimer FE, Counsell SJ, Murgasova M, Aljabar P, Nunes RG, Larkman DJ, Rees G, Edwards AD 2010 Emergence of resting state networks in the preterm human brain. Proc Natl Acad Sci U S A 107:20015-20020.

46. Smyser CD, Inder TE, Shimony JS, Hill JE, Degnan AJ, Snyder AZ, Neil JJ 2010 Longitudinal analysis of neural network development in preterm infants. Cereb Cortex 20:2852-2862.

47. Fransson P, Skiöld B, Engström M, Hallberg B, Mosskin M, Aden U, Lagercrantz H, Blennow M 2009 Spontaneous brain activity in the newborn brain during natural sleep--an fMRI study in infants born at full term. Pediatr Res 66:301-305.

48. Fransson P, Skiöld B, Horsch S, Nordell A, Blennow M, Lagercrantz H, Aden U 2007 Resting-state networks in the infant brain. Proc Natl Acad Sci U S A 104:15531-15536.

49. White BR, Liao SM, Ferradal SL, Inder TE, Culver JP 2012 Bedside optical imaging of occipital resting-state functional connectivity in neonates. Neuroimage 59:2529-2538.

50. Lawn J, Shibuya K, Stein C 2005 No cry at birth: global estimates of intrapartum stillbirths and intrapartum-related neonatal deaths. Bull World Health Organ 83:409-417.

51. Volpe JJ 2001 Perinatal brain injury: from pathogenesis to neuroprotection. Ment Retard Dev Disabil Res Rev 7:56-64.

52. Cooper RJ, Hebden JC, O'Reilly H, Mitra S, Michell AW, Everdell NL, Gibson AP, Austin T 2011 Transient haemodynamic events in neurologically compromised infants: a simultaneous EEG and diffuse optical imaging study. Neuroimage 55:1610-1616.

53. Hellstrom-Westas L, Rosen I 2010 Electroencephalography and amplitude-integrated EEG. In Lagercrantz H (ed) The Newborn Brain: Neuroscience and Clinical Applications. Cambridge University Press, pp 211-228.

54. Lewis LD, Ching S, Weiner VS, Peterfreund RA, Eskandar EN, Cash SS, Brown EN, Purdon PL 2013 Local cortical dynamics of burst suppression in the anaesthetized brain. Brain 136:2727-2737.

55. Chalia M, Lee CW, Dempsey LA, Edwards AD, Singh H, Michell AW, Everdell NL, Hill RW, Hebden JC, Austin T, Cooper RJ 2016 Hemodynamic response to burst-suppressed and discontinuous electroencephalography activity in infants with hypoxic ischemic encephalopathy. Neurophotonics 3:10.

56. Torricelli A, Contini D, Pifferi A, Caffini M, Re R, Zucchelli L, Spinelli L 2014 Time domain functional NIRS imaging for human brain mapping. Neuroimage 85 Pt 1:28-50.

57. Hebden JC, Gibson A, Yusof RM, Everdell N, Hillman EM, Delpy DT, Arridge SR, Austin T, Meek JH, Wyatt JS 2002 Three-dimensional optical tomography of the premature infant brain. Phys Med Biol 47:4155-4166.

58. Austin T, Gibson AP, Branco G, Yusof RM, Arridge SR, Meek JH, Wyatt JS, Delpy DT, Hebden JC 2006 Three dimensional optical imaging of blood volume and oxygenation in the neonatal brain. Neuroimage 31:1426-1433.

59. Hintz SR, Benaron DA, van Houten JP, Duckworth JL, Liu FW, Spilman SD, Stevenson DK, Cheong WF 1998 Stationary headband for clinical time-of-flight optical imaging at the bedside. Photochem Photobiol 68:361-369.

60. Hintz SR, Cheong WF, van Houten JP, Stevenson DK, Benaron DA 1999 Bedside imaging of intracranial hemorrhage in the neonate using light: comparison with ultrasound, computed tomography, and magnetic resonance imaging. Pediatr Res 45:54-59.

61. Hebden JC, Gibson A, Austin T, Yusof RM, Everdell N, Delpy DT, Arridge SR, Meek JH, Wyatt JS 2004 Imaging changes in blood volume and oxygenation in the

newborn infant brain using three-dimensional optical tomography. Phys Med Biol 49:1117-1130.

62. Gibson AP, Austin T, Everdell NL, Schweiger M, Arridge SR, Meek JH, Wyatt JS, Delpy DT, Hebden JC 2006 Three-dimensional whole-head optical tomography of passive motor evoked responses in the neonate. Neuroimage 30:521-528.

63. Brigadoi S, Ceccherini L, Cutini S, Scarpa F, Scatturin P, Selb J, Gagnon L, Boas DA, Cooper RJ 2013 Motion artifacts in functional near-infrared spectroscopy: A comparison of motion correction techniques applied to real cognitive data. Neuroimage.

64. Barker JW, Rosso AL, Sparto PJ, Huppert TJ 2016 Correction of motion artifacts and serial correlations for real-time functional near-infrared spectroscopy. Neurophotonics 3:031410.

65. Gu Y, Han J, Liang Z, Yan J, Li Z, Li X 2016 Empirical mode decomposition-based motion artifact correction method for functional near-infrared spectroscopy. J Biomed Opt 21:15002.

66. Gagnon L, Perdue K, Greve DN, Goldenholz D, Kaskhedikar G, Boas DA 2011 Improved recovery of the hemodynamic response in diffuse optical imaging using short optode separations and state-space modeling. Neuroimage 56:1362-1371.

67. Saager R, Berger A 2008 Measurement of layer-like hemodynamic trends in scalp and cortex: implications for physiological baseline suppression in functional near-infrared spectroscopy. J Biomed Opt 13:034017.

68. Gregg NM, White BR, Zeff BW, Berger AJ, Culver JP 2010 Brain specificity of diffuse optical imaging: improvements from superficial signal regression and tomography. Front Neuroenergetics 2.

69. Markham J, White BR, Zeff BW, Culver JP 2009 Blind identification of evoked human brain activity with independent component analysis of optical data. Hum Brain Mapp 30:2382-2392.

70. Zhang H, Zhang YJ, Lu CM, Ma SY, Zang YF, Zhu CZ 2010 Functional connectivity as revealed by independent component analysis of resting-state fNIRS measurements. Neuroimage 51:1150-1161.

71. Franceschini MA, Joseph DK, Huppert TJ, Diamond SG, Boas DA 2006 Diffuse optical imaging of the whole head. J Biomed Opt 11:054007.

72. Zhang Y, Brooks DH, Franceschini MA, Boas DA 2005 Eigenvector-based spatial filtering for reduction of physiological interference in diffuse optical imaging. J Biomed Opt 10:11014.

73. Virtanen J, Noponen T, Merilainen P 2009 Comparison of principal and independent component analysis in removing extracerebral interference from near-infrared spectroscopy signals. J Biomed Opt 14:054032.

74. Brigadoi S, Aljabar P, Kuklisova-Murgasova M, Arridge SR, Cooper RJ 2014 A 4D neonatal head model for diffuse optical imaging of pre-term to term infants. Neuroimage 100:385-394.

75. Ferradal SL, Eggebrecht AT, Hassanpour M, Snyder AZ, Culver JP 2014 Atlas-based head modeling and spatial normalization for high-density diffuse optical tomography: in vivo validation against fMRI. Neuroimage 85 Pt 1:117-126.

76. Cooper RJ, Caffini M, Dubb J, Fang Q, Custo A, Tsuzuki D, Fischl B, Wells W, Dan I, Boas DA 2012 Validating atlas-guided DOT: a comparison of diffuse optical tomography informed by atlas and subject-specific anatomies. Neuroimage 62:1999-2006.

77. Tak S, Ye JC 2014 Statistical analysis of fNIRS data: a comprehensive review. Neuroimage 85 Pt 1:72-91.

78. Friston KJ, Holmes AP, Poline JB, Grasby PJ, Williams SC, Frackowiak RS, Turner R 1995 Analysis of fMRI time-series revisited. Neuroimage 2:45-53.

79. Ye JC, Tak S, Jang KE, Jung J, Jang J 2009 NIRS-SPM: statistical parametric mapping for near-infrared spectroscopy. Neuroimage 44:428-447.

80. Hassanpour MS, White BR, Eggebrecht AT, Ferradal SL, Snyder AZ, Culver JP 2014 Statistical analysis of high density diffuse optical tomography. Neuroimage 85 Pt 1:104-116.

81. Huppert TJ 2016 Commentary on the statistical properties of noise and its implication on general linear models in functional near-infrared spectroscopy. Neurophotonics 3:010401.

82. Chitnis D, Airantzis D, Highton D, Williams R, Phan P, Giagka V, Powell S, Cooper RJ, Tachtsidis I, Smith M, Elwell CE, Hebden JC, Everdell N 2016 Towards a wearable near infrared spectroscopic probe for monitoring concentrations of multiple chromophores in biological tissue in vivo. Rev Sci Instrum 87:065112.

83. Amal Kassab and Jr, me Le Lan and Phetsamone Vannasing and Mohamad S 2015 Functional near-infrared spectroscopy caps for brain activity monitoring: a review. Appl. Opt. 54:576--586.

References for Figures

Figure 2b: Hillman EM. Optical brain imaging in vivo: techniques and applications from animal to man. J Biomed Opt 2007;12:051402.

Figure 3a: Singh H, Cooper RJ, Wai Lee C, et al. Mapping cortical haemodynamics during neonatal seizures using diffuse optical tomography: A case study. Neuroimage Clin 2014;5:256-65.

Figure 3b: Singh H, Cooper RJ, Wai Lee C, et al. Mapping cortical haemodynamics during neonatal seizures using diffuse optical tomography: A case study. Neuroimage Clin 2014;5:256-65.

Figure 3e: Brigadoi S, Aljabar P, Kuklisova-Murgasova M, Arridge SR, Cooper RJ. A 4D neonatal head model for diffuse optical imaging of pre-term to term infants. Neuroimage 2014;100:385-94.

Figure 3f: Brigadoi S, Aljabar P, Kuklisova-Murgasova M, Arridge SR, Cooper RJ. A 4D neonatal head model for diffuse optical imaging of pre-term to term infants. Neuroimage 2014;100:385-94.

Figure 4: Ferradal SL, Liao SM, Eggebrecht AT, et al. Functional Imaging of the Developing Brain at the Bedside Using Diffuse Optical Tomography. Cereb Cortex 2016;26:1558-68.

Figure 5: Cooper RJ, Hebden JC, O'Reilly H, et al. Transient haemodynamic events in neurologically compromised infants: a simultaneous EEG and diffuse optical imaging study. Neuroimage 2011;55:1610-6.

Figure 6: Singh H, Cooper RJ, Wai Lee C, et al. Mapping cortical haemodynamics during neonatal seizures using diffuse optical tomography: A case study. Neuroimage Clin 2014;5:256-65.

Figure 7b: Austin T, Gibson AP, Branco G, et al. Three dimensional optical imaging of blood volume and oxygenation in the neonatal brain. Neuroimage 2006;31:1426-33.

Figure 7c: Austin T, Gibson AP, Branco G, et al. Three dimensional optical imaging of blood volume and oxygenation in the neonatal brain. Neuroimage 2006;31:1426-33.

Figure Legends

Figure 1

A decision tree that provides a definition of the different forms of diffuse optical monitoring. While nomenclature varies across the field, these are the definitions preferred by the authors.

Figure 2

(a) The absorption properties of oxy- (red line), deoxyhemoglobin (green line) and water (blue line) in biological tissue. In the optical window (shaded in blue) between 700 and 900 nm, light is relatively transparent as the absorption by water molecules is relatively low compared to oxy- and deoxyhemoglobin.

(b) The path of near-infrared light from an optical source follows a banana-shape as it travels in cerebral tissue before the transmitted light is measured at the detector.

(c) The UCL Optical Imaging System (Gowerlabs, London). This is a continuous wave device that samples at 10Hz and provides 16 optical sources and 16 detectors.

(d) An example of headgear design used in infant studies of whole-head diffuse optical tomography.

Figure 3

Diffuse Optical Tomography Image Reconstruction

(a) A photo of the headgear used in infant whole-head diffuse optical tomography scanning.

(b) A schematic of the locations of sources (red dots) and detectors (blue dots) of the headgear in (a). The black lines represent source-detector channels.

(c) During scanning, raw light intensity data is converted to changes in optical density and these are assigned to the location of the source-detector channels of the headgear array.

(d) An anatomical MRI is required to provide structural information for image reconstruction. This can either be the infant's own MRI or an age-matched atlas may be used.

(e) The anatomical MRI image is segmented to identify the different tissue types (such as scalp, cerebrospinal fluid, gray matter, white matter) as these will have different optical properties.

(f) A mathematical model of how light will travel through brain tissue is derived. This will define how light intensity measured at a detector will change given localized changes in oxy- and deoxyhemoglobin.

(g) A sensitivity matrix describing how the changes in light intensity at each channel location (from b) relates to the changes in oxy- and deoxyhemoglobin concentration (the final desired image) can be calculated using the model of light propagation in tissue from (f).

(h) The desired image is reconstructed by combining the properties of the sensitivity matrix (g) with the channel data (c).

Figure 4

Resting state functional connectivity maps from a single healthy term infant. The first column indicates the regions of interest selected for seed-based analysis of the visual (vis), middle temporal (MT) and primary auditory (A1) networks. The second column displays the correlation maps (i.e. networks) for each region of interest from functional connectivity diffuse optical tomography (fcDOT). The oxyhemoglobin signal (ΔHbO_2) from DOT is overlaid on the subject-specific anatomical MRI image. The third column displays the correlation maps for each region of interest using the blood oxygen level dependent (BOLD) signal in fMRI.

Figure 5

DOT images reconstructed from a neurologically compromised infant for a single hemodynamic event. The series of images are reconstructed at a depth of 9-12 mm from the left lateral surface at 95 s preceding, to 95 s after the event. Red indicates an increase, and blue a decrease in the concentration of oxyhemoglobin.

Figure 6

DOT images reconstructed in an infant with severe hypoxic ischemic encephalopathy. The upper graph illustrates the oxy- (HbO, red line), deoxy- (HbR, blue line) and total hemoglobin (HbT, green line) changes for a seizure event identified by electroencephalography (EEG), which was recorded simultaneously. The numbered images below represent the cortical changes in 3 different views (dorsal, left and right lateral) seen during the different time points of the seizure event as depicted in the graph. Red indicates an increase, and blue a decrease in the total hemoglobin (HbT) concentration in the DOT images.

Figure 7

(a) A photo of the UCL time-domain DOT system (MONSTIR II) in the Rosie Hospital, Cambridge, UK.

(b) A cranial ultrasound of a preterm infant revealing a left sided intraventricular hemorrhage and hemorrhagic parenchymal infarct.

(c) A 3D-DOT image taken at a coronal section of the same preterm infant showing regional blood volume (left) and oxygen saturation (right). There is an increase in hemoglobin concentration and decrease in oxygen saturation in the area corresponding to the hemorrhage and infarct.

Diffuse Optical Tomography to Investigate the Newborn Brain

Chuen Wai Lee[1,2], Robert J Cooper[1,3], Topun Austin[1,2]

1. neoLAB, The Evelyn Perinatal Imaging Centre, The Rosie Hospital, Cambridge University Hospitals NHS Foundation Trust, Cambridge, United Kingdom, 2. Department of Neonatology, The Rosie Hospital, Cambridge University Hospitals NHS Foundation Trust, Cambridge, United Kingdom, 3. Department of Medical Physics and Biomedical Engineering, University College London, London, United Kingdom.

Running Title

Diffuse Optical Tomography in Newborns

Corresponding author

Topun Austin Email: topun.austin@addenbrookes.nhs.uk

Department of Neonatology, The Rosie Hospital, Cambridge University Hospitals NHS Foundation Trust, Cambridge Biomedical Campus, Hills Road, Cambridge, CB2 0QQ, UK

Tel: 01223 256947

Conflict of Interest Statement

The authors have no conflicts of interest relevant to this article to disclose.

Funding

This work was supported by the Medical Research Council, London UK (MR/L017490/1), the Evelyn Trust, Cambridge UK (09/26 2013 RTF) and the Engineering and Physical Sciences Research Council, London UK (EP/N025946/1).

Word Count

Manuscript: ~~4218~~ 4602 words

Abstract: 134 words

Abstract

Over the past 15 years, functional near-infrared spectroscopy (fNIRS) has emerged as a powerful technology for studying the developing brain. Diffuse Optical Tomography (DOT) is an extension of fNIRS that combines hemodynamic information from dense optical sensor arrays over a wide field of view. Using image reconstruction techniques, DOT can provide images of the hemodynamic correlates to neural function that are comparable to those produced by functional MRI (fMRI).

This review article explains the principles of DOT, and ~~provides an overview of~~highlights the growing literature on the use of DOT in the study of healthy development of the infant brain, and the study of novel pathophysiology in infants with brain injury. Current challenges, particularly around instrumentation and image reconstruction, will be discussed as will the future of this growing field, with particular focus on whole-brain, time-resolved DOT.

Introduction

The field of medical physics and biomedical engineering has provided a range of novel neuroimaging techniques that have enabled scientists and clinicians to investigate the functional organization and architecture of the human brain in health and disease. In recent years, functional near-infrared spectroscopy (fNIRS) has become an increasingly valuable tool. As well as being non-invasive, relatively low-cost and easy to set up, it can be carried out in infants who are awake and do not need to be transported to specialized imaging facilities. Diffuse optical tomography (DOT) is a natural extension of fNIRS, which combines multichannel data acquisition with image reconstruction software to provide images of changes in regional blood volume and oxygenation at high temporal and spatial resolution. This technology is increasingly being used by researchers and clinicians to study healthy brain development as well as pathophysiology in critically ill infants in intensive care. Figure 1 summarizes the terminology and NIRS domains that will be described in this paper.

The aim of this paper is to explain the principles of DOT and ~~provide an overview of existing literature~~highlight studies using DOT in newborn infants. We also summarize the current challenges of the technique and discuss the future of the field, with particular emphasis on technological developments and time-domain DOT techniques.

Principles of Optical Imaging

Near-Infrared Spectroscopy (NIRS)

Near-infrared spectroscopy (NIRS) is a non-invasive tissue monitoring technique that exploits the relative transparency of biological tissue to near-infrared light (650-950nm) and

the wavelength dependent absorption characteristics of light absorbing compounds, or chromophores. In the brain, haemoglobin is the dominant chromophore, whose absorption varies with oxygenation, first described by Jöbsis in 1977 (1-3) (Figure 2a).

However, the dominant interaction between near-infrared light and tissue is not absorption but scattering, such that the path travelled by a given photon will constitute a 'random walk': bouncing randomly from one scattering event to the next. Near-infrared light therefore forms a *diffuse* field when entering tissue. Assuming scattering remains constant, loss of light, or attenuation, will be due to changes in absorption by the main chromophores (light absorbing molecules). The simplest form of NIRS measurement consists of two wavelengths of NIR light, coupled into tissue via an optical fiber positioned a few centimetres away to collect light and transmit it to a detector. This method has been used extensively to study cerebral oxygenation in the newborn infant (4, 5) (for a review see (6)).

Formatted: Font: Times New Roman, Italic, English (U.S.)

Functional Near-Infrared Spectroscopy (fNIRS)

During cortical activation, neural excitation produces an increased metabolic demand that results in local changes in oxygen consumption, vasodilatation, increased blood flow and increased oxygenation. This relationship, between neural activity and vasodilation, is known as neurovascular coupling. In adults, a local increase in neural activity is typically characterized by an increase in oxyhemoglobin concentration and a decrease in deoxyhemoglobin concentration, due to the rapid influx of oxygenated blood (7, 8). While the exact mechanisms of neurovascular coupling are still a matter of active investigation, the consistency of the functional hemodynamic response means that it provides an effective indirect measure of cortical function. As NIRS is able to monitor changes in the concentration of oxy- and deoxy-hemoglobin, the technique can be used to measure the functional hemodynamic response to specific stimuli. This technique is known as functional

NIRS or fNIRS. The same physiological principles exploited by fNIRS underpin the blood oxygen level dependent (BOLD) signal, which is used in functional MRI (fMRI). However, while the BOLD signal is predominantly sensitive to the concentration of deoxyhemoglobin (9), fNIRS methods have the advantage of being able to monitor the concentrations of both oxy- and deoxy-hemoglobin independently, which significantly aids the physiological interpretation of fNIRS measurements.

In infants, the maturity of neurovascular coupling is still in question, and studies have yielded adult-like responses (10-12), inverted (decreased oxyhaemoglobin and increased deoxyhaemoglobin) responses (13) or a mixture of the two (14, 15). Although the nature of this response remains controversial (and is beyond the scope of this review), hemodynamic changes that are temporally correlated to the external stimulus can still provide an indication of neural activation, and the interpretation of response polarity should be carefully assessed depending on the nature of the subject or study.

Early Application of fNIRS in Infants

Early infant functional studies typically used a single source and detector providing one channel i.e. one measurement of ~~to measure~~ the cortical changes in a primary area of interest (14, 16, 17). However, the majority of commercial fNIRS systems now employ numerous source and detector fibers into an array that provides multiple fNIRS channels facilitating the examination of extended cortical regions. The most widely used multi-channel systems are continuous wave (CW) devices, which are relatively low cost and simple to set up (for review of CW systems see (18)).

Multi-channel CW systems measure light attenuation by continuous illumination of the head with multiple sources. To distinguish which source gave rise to the light measured at any given detector, either time or frequency multiplexing methods must be used. In time multiplexing, each source is illuminated in turn for a specific period of time, so that the origin of any detected light is always apparent. In frequency multiplexing, all the sources are illuminated continuously, but with each source modulated at a distinct frequency. CW systems typically allow a sampling rate from 5 to 100 Hz, providing accurate temporal information on cortical hemodynamic activity (19).

Two-Dimensional Mapping and Optical Topography

The simplest approach to obtaining images of spatial variation of brain activity using near-infrared methods is to create a two-dimensional map of the responses obtained using multi-channel CW fNIRS devices. These two-dimensional representations can be generated by interpolating the signal measured by multiple fNIRS channels across the interrogated area (20, 21). This approach is often referred to as optical topography. While this technique has helped accelerate our understanding of neurodevelopment and cognition in the infant brain, including language (22-25), vocal (26, 27), social (28) and face (29) perception (for more reviews (30-33)), the anatomical registration and spatial resolution of the resulting images is ~~severely~~ limited, and the quantitative accuracy of the images can be ~~severely~~ compromised (34). It is important to note, however, that significant functional information can be obtained without absolute quantification; fMRI is rightly considered the gold-standard in functional neuroimaging, but in most common applications it remains purely qualitative (35).

Diffuse Optical Tomography

Diffuse optical tomography (DOT) enables the production of three-dimensional images. The term "diffuse" describes the path of near-infrared light when it enters tissue (as explained in the "Principles of Optical Imaging" section). Unlike 2D topographic approaches, DOT exploits measurements from multiple overlapping channels, with ~~varying~~ a range of source-detector distances to obtain depth information. ~~Therefore a~~A major advantage of this approach is the ability to separate hemodynamics occurring at different depths, and thus reduce the influence of blood oxygenation changes in extracerebral tissues such as the scalp or skull (see section titled "Physiological signal contamination").

The quality of DOT images is dependent on the number of channels that sample a given volume of tissue. The total number of channels one can achieve is dependent on the size and weight of the optical fibers and the number of source and detectors available in a DOT system. While a sparse array can provide whole-head coverage (36), the resulting spatial resolution can be compromised. At present, commercial devices that can perform DOT (Figure 2c) provide 10-20 sources and 10-20 detectors, which allow imaging of sub-sections of the adult cortex, or the majority of the infant cortex. Image resolution is a function of array density, such that dense arrays provide better spatial resolution (37). However, no DOT system (commercially available or otherwise) ~~system can~~has yet been demonstrated ~~provide~~ that can provide dense sampling ~~-~~(i.e. with a nearest-neighbor source detector separation of < ~~20~~ 15 mm) ~~over~~ over the whole ~~head~~ scalp of either the infant or the adult (38).

DOT Image Reconstruction

DOT image reconstruction is an example of an inverse problem, in which the goal is to determine internal features of an object using measurements of light transmitted between points on the surface. DOT image reconstruction is ill-posed and highly under-determined.

Ill-posed, meaning that many different internal configurations could equally explain the measurements made at the surface (i.e. there is not a unique solution) and highly underdetermined, meaning that the number of unknowns (i.e. voxels in our image) far exceeds the number of measurements made at the surface. One approach to simplify this problem is to produce images of a difference between two points in time, rather than to attempt to create images of the absolute optical properties of the brain. By assuming the changes that have occurred between these two time points are small relative to the background optical characteristics of the tissue, the DOT reconstruction problem can be linearized, significantly simplifying the mathematical challenge (39). A schematic of DOT image reconstruction is shown in Figure 3 and for a more complete summary see (39-41).

Application of DOT in the Newborn Brain

The earliest infant DOT images were reconstructed in the late 1990s. For example, hemodynamic changes over the sensorimotor regions were demonstrated in the premature infant cortex by Chance et al. (42) using a system consisting of nine sources and four detectors. ~~The first application of DOT imaging in the newborn brain was demonstrated by~~ Hintz et al. (13) reconstructed functional images of passive arm movements over the motor cortex in preterm infants using an array with 9 sources and 16 detectors providing 144 independent measurements or channels~~. The array was placed over the motor cortex in preterm infants and functional images of passive arm movements were reconstructed, demonstrating an increase in blood volume over the activated region~~.

~~Aside from this early pioneering study, only~~ More recently ~~has~~ the neonatal application of DOT become more widespread.

In a study of healthy newborn infants, Liao et al. used a CW high-density DOT system to image functional activation of the primary visual cortex (43). To counteract the effect of superficial haemodynamic signals from the extra-cerebral tissue, superficial signal regression between the first- and second-nearest source detector paired channels was carried out. Bilateral increases in oxyhemoglobin concentration were apparent in response to visual stimuli in the reconstructed DOT images. A direct comparison of the hemodynamic response in the DOT images was carried out with the conventionally recorded hemodynamic changes in the source-detector channels. This demonstrated an increase in the signal-to-noise ratio of the DOT images by two-fold compared to the channel-wise data.

Intrinsic brain activity at rest in the absence of a stimulus can also provide information on functional cerebral development. This field, originally established using the BOLD signal in fMRI research, is known as resting state functional connectivity (RSFC) (44) and RSFC networks characterized by bilateral cortical connectivity have been described in the term and preterm infant (45-48).

Focusing on the visual cortex, White et al. produced the first DOT images of bilateral occipital connectivity at rest ~~resting state networks~~ in preterm and full-term born infants (49). An array consisting of 18 sources and 16 detectors was placed over the occipital cortex to record resting-state brain activity for up to 20 minutes. To identify ~~functional~~ connectivity ~~in the resting state~~, two standard approaches: seed-based analysis and independent component analysis (ICA) were carried out on the DOT images. Visual networks with bilateral connectivity between both cerebral hemispheres in the visual cortex were identified in the full-term and healthy preterm groups. Interestingly, one preterm subject with a diagnosis of a

left occipital infarct displayed unilateral connectivity only demonstrating the sensitivity of DOT to cerebral pathology.

In a recent study, Ferradal et al. also identified ~~resting-state networks~~bilateral cortical connectivity in the resting-state in healthy full-term born infants using both fMRI and DOT imaging modalities in the same subjects for the first time (38). DOT resting-state data were recorded for up to 60 minutes using a dense array of 32 sources and 34 detectors over the temporal and occipital cortices. MRI scans were performed within a day following DOT scanning and subject-specific structural MRI head models of light propagation were used. Using seed-based analysis and ICA, the DOT ~~RSFC maps~~images revealed bilateral connectivity in the visual, middle temporal and primary auditory networks. Comparisons between the DOT and fMRI seed based maps confirmed strong qualitative and quantitative agreement (Figure 4).

Application of DOT to Investigate Infant Pathology

Perinatal hypoxic ischemic encephalopathy (HIE) is a major cause of mortality and neurodevelopmental disability in term infants (50) resulting from severe perinatal deficit in cerebral blood flow and oxygen delivery (51). Subsequent brain injury is clinically characterized by seizure activity and abnormal neurological function, which may be associated with hemodynamic changes. DOT can offer valuable information on cerebral hemodynamics and oxygenation associated with brain injury, which are currently not available in the clinical setting. In a simultaneous EEG and DOT study of neurologically compromised infants, large transient hemodynamic events were identified in a small group of newborn infants diagnosed with clinical symptoms of seizures (52). Hemodynamic events

were characterized by a slow increase in oxyhemoglobin followed by a rapid decrease before a slow return to baseline (Figure 5).

In a case study using EEG and DOT, Singh et al. reported the first DOT images of hemodynamic responses to electrographic seizures in an infant with severe HIE (36). A flexible head cap with 11 EEG electrodes, and 16 sources and 16 detectors was used to record 60-minutes of data that contained 7 electrographic seizure events lasting 30 – 90 s. Although there was spatial variation, the DOT images revealed an initial small increase in cortical blood volume followed by a profound and extended decrease lasting several minutes (Figure 6).

In the absence of electrographic seizures, HIE infants may experience electrographic burst suppression which is associated with poor neurodevelopmental prognosis (53). These patterns present as low-voltage electrical activity alternating with sharp high-voltage bursts that occur globally or in focal cortical regions (54). Neuroimaging strategies with improved spatial specificity compared to EEG can provide close monitoring of this pathological state. Using the same flexible DOT-EEG cap array (36), Chalia et al. identified hemodynamic responses relating to electrographic burst events of 4-6 s, in 6 infants with HIE (55). The DOT images demonstrated a decrease in oxyhemoglobin prior to, or during burst activity, followed by a large increase and a return to baseline with an undershoot. Patient-specific spatial patterns that were not apparent in the EEG were observed in the DOT images signifying the complex morphology of burst suppression.

Time-domain DOT

In addition to CW devices which measure only the changes in intensity of the detected light, and are thus unable to separate the effects of absorption and scatter or provide absolute quantification of tissue parameters, researchers have developed what are known as time-resolved or time-domain DOT devices (TD-DOT). TD devices operate by injecting very short pulses of light (picoseconds) in to tissue and measuring the time-of-flight of individual photons using highly sensitive, photon-counting detectors (for review of TD methods, see (56)). By building up a histogram of photon flight-times, TD-DOT provides a rich data set that contains information related to both the absorption and scattering properties of the underlying tissue. As a result, TD-DOT requires fewer assumptions to be made than CW methods, and it is possible to obtain absolute measurements of oxy- and deoxy-hemoglobin concentrations.

Because TD-DOT employs sensitive photon-counting detectors, it is also possible to make measurements over much larger source-detector distances including across the whole newborn infant head, allowing the creation of DOT images of the entire volume of the infant brain. Early images reconstructed using this technique were able to identify intracranial hemorrhages in preterm infants ~~The first whole head TD-DOT images reconstructed for a preterm infant demonstrated clear hemodynamic inhomogeneities associated with a large unilateral intracranial hemorrhage~~(57-59) (for an example see Figure 7). Compared with established imaging techniques such as ultrasound, blinded comparisons of DOT images in infants of varying gestation were interpreted as correct in six out of eight cases using TD-DOT (60). Hemodynamic changes induced by adjusting mechanical ventilator settings in a full-term infant with HIE (61) have also been imaged across the whole brain ~~using TD-DOT~~, as have functional hemodynamic changes in the somato-motor cortex during passive arm movement in healthy preterm infants (62).

Formatted: Font: (Default) Times

Continuing Challenges of DOT

Recent advances in DOT have allowed the technique to become an effective method for the investigation of both healthy and pathological neurodevelopment. However, as with all emerging technologies, a number of significant challenges still remain.

Head-gear Array Design

Due to the physical size and weight of optical fibers, and the number of optodes available in a DOT system, the maximum number that can be used is ~~always~~ currently limited, particularly for small infants. As a result, i~~I~~nvestigators employing DOT must still choose between a sparse whole-head array (36) or a high-density localized array (38). The ability to flexibly design an array to suit a given experiment can be extremely beneficial, but t~~T~~he lack of a single 'catch-all' array solution does ~~makes DOT more challenging for users,~~ make~~s~~ it harder to perform quantitative cross-study comparisons and also hinders the standardization and automation of data processing methods. ~~continues to hold back the advance of DOT methodologies in both clinical and neuroscientific applications.~~

Movement Artifacts

~~Like infant studies, movement can be a significant problem in DOT.~~Movement can be a significant problem in DOT studies, particularly in awake infants. Relative motion between the optical fibre and the scalp of the subject will affect optical coupling, which will often cause large variations in the measured optical intensity. Typically, the impact of movement on DOT data is to invoke transient, high-amplitude spikes in intensity, which immediately subside when the movement ends. Because these artifacts are temporary, periods of good-quality data DOT can usually be extracted, even in studies of awake infants. Unlike with

fMRI, it is therefore rare that a whole DOT data set will have to be discarded due to movement artifacts. ~~studies using DOT as well as using fMRI and EEG.~~ There are three broad strategies that can be employed to address the problem of motion in DOT. The first is to prevent motion artifacts from occurring at all; by encouraging the infant to sleep, for example by feeding and swaddling the infant; by ensuring that there are appropriate stimuli to engage an awake infant; and to construct the optode array headgear to optimize the coupling of the optodes to the head. The second is to exclude data that is deemed (by visual inspection or via the use of an accelerometer or video recording) to be contaminated by motion artifact and the third is to use post-processing methods to clean the data to remove the effects of motion (63). In practice, most DOT studies employ all three of these approaches, while NIRS and DOT motion artifact filtering methodologies continue to advance (64, 65). ~~, but motion artifact remain a challenge, particularly in infants~~with success and further research in this field can help enhance DOT images~~.~~

Physiological signal contamination

One technical limitation common to all forms of NIRS and DOT is contamination of the measured signal by non-neuronal sources. These include systemic hemodynamic changes in both the brain and the superficial layers of the head including the skin caused by the cardiac cycle, blood pressure and respiration. Because of the ability of DOT to obtain 3D information, DOT image reconstruction can inherently separate the scalp and brain layers. Simple approaches employed in NIRS can also be used for DOT, including low-pass filtering of the signal and block averaging to extract the signal that is temporally correlated to an external functional stimulus (18). More recent multivariate techniques, such as superficial signal regression (66-68), which uses short source-detector channels to measure scalp signal, and independent component analysis (ICA) (69, 70) or principal component analysis (PCA)

{Zhang, 2010, Noninvasive functional and structural connectivity mapping of the human thalamocortical system;Franceschini, 2006, Diffuse optical imaging of the whole head;Franceschini, 2006 #113;Franceschini, 2006 #113}, (71-73), have been developed to isolate cerebral signals.

Structural Priors

A major advantage of DOT in comparison to fMRI is its portability. However accurate DOT image reconstruction requires high-quality structural models of the subject's head to act as a prior for image reconstruction. Significant efforts have therefore been made to optimize an age-matched 4D neonatal head model (74) using MRI head atlases as an alternative to subject-specific data (36, 49, 55). An advantage of using a standard atlas is that it facilitates group comparisons across subjects, as it defines a common coordinate space (75) although this reduces the spatial specificity of the DOT images (76). Careful application of the optode array, and measurement of its position relative to certain cranial landmarks using a 3D digitizer can minimize the errors associated with registration and positioning and yield high-quality, anatomically registered DOT images.

Statistical Analysis

As an emerging field, there is as yet no gold-standard approach for determining statistical significance or inference from DOT images (for general review see (77)). To extract the functional response to certain stimuli, event related designs have used a general linear model (GLM) approach to model the hemodynamic changes as a linear combination of independent variables (78). Similar to fMRI analysis, statistical parametric mapping (SPM) tools that use a GLM approach have also been developed and implemented for the statistical analysis of topographic ~~maps~~(79) and ~~in DOT statistical analysis~~tomographic images (80). However,

there remain some concerns regarding the application of fMRI data processing methodologies to DOT because of the fundamentally different noise characteristics of the two data-types (81). —A major bottle-neck in achieving a standardized (or even automated) DOT image reconstruction and processing pipeline is the lack of a 'catch-all' high-density, whole-scalp imaging array.

Future Directions

One of the major confounding limitations of DOT methods remains the necessity of using large numbers of optical fibers. However, technology is rapidly developing that will allow DOT imaging without the use of optical fibres. Lightweight electronics can be worn by a subject with fewer cables in recent 'wearable' fNIRS systems enabling researchers to study mobile adult subjects (19, 82, 83). ~~This year~~ Chitnis et al. (82) published the first functional images of the human brain obtained with a fibreless, high-density DOT system. Though designed for adults, this technology will likely be adapted for studies of the infant brain. By dispensing with the optical fibers, it may soon be possible to produce a we~~r~~arable, high-density, whole-scalp DOT system that will provide~~obtain~~ high-quality functional images of the infant brain continuously at the bedside~~, which~~

This has significant implications for both developmental neuroscience and clinical practice. For example, this would allow continuous monitoring of resting state cortical connectivity in premature infants as a measurement of cognitive development or the detection of pathological cortical regions such as in stroke.

While these wearable technologies are impressive, they are still CW devices, and thus provide limited quantitation. Historically, TD systems have been large and extremely

expensive because of the complex electronics required for photon-counting. The advent of low-cost, solid-state single photon avalanche detectors (SPADs), which are now being developed for a range of novel time-of-flight technologies, will allow the issues of size and cost to be minimized in future generations of instruments (56). It is now reasonable to predict that fibreless TD-DOT technologies that provide quantitative, depth-sensitive, 3D images of the whole infant brain with a resolution of ~5 mm will be available within the next decade.

Conclusions

From the early measurements of cerebral oxygenation in newborns, to the more complex images of functional brain activity in recent years, DOT is rapidly emerging as an important tool for clinicians and neuroscientists to investigate the newborn brain. As the field has grown, so too has the expectation of the technology, and new challenges have arisen as we continue to push the boundaries of DOT. Wearable technologies are now emerging, which have the potential to allow continuous imaging of infant brain function at the cot-side within the next few years. Innovations in TD-DOT technology imply that clinical TD-DOT systems are now on the horizon. As the technology advances, we must ensure that DOT is given the opportunity to become a clinically useful methodology; one that will provide clinicians with continuous measures of cerebral oxygenation, brain function and neurodevelopment that will complement neonatal intensive care.

References

1. Jöbsis FF 1977 Noninvasive, infrared monitoring of cerebral and myocardial oxygen sufficiency and circulatory parameters. Science 198:1264-1267.
2. van der Zee P, Cope M, Arridge SR, Essenpreis M, Potter LA, Edwards AD, Wyatt JS, McCormick DC, Roth SC, Reynolds EO 1992 Experimentally measured optical pathlengths for the adult head, calf and forearm and the head of the newborn infant as a function of inter optode spacing. Adv Exp Med Biol 316:143-153.
3. Matcher SJ, Cope M, Delpy DT 1994 Use of the water absorption spectrum to quantify tissue chromophore concentration changes in near-infrared spectroscopy. Phys Med Biol 39:177-196.
4. Brazy JE, Lewis DV, Mitnick MH, Jöbsis vander Vliet FF 1985 Noninvasive monitoring of cerebral oxygenation in preterm infants: preliminary observations. Pediatrics 75:217-225.
5. Wyatt JS, Cope M, Delpy DT, Wray S, Reynolds EO 1986 Quantification of cerebral oxygenation and haemodynamics in sick newborn infants by near infrared spectrophotometry. Lancet 2:1063-1066.
6. Wolf M, Greisen G 2009 Advances in near-infrared spectroscopy to study the brain of the preterm and term neonate. Clin Perinatol 36:807-834, vi.
7. Obrig H, Villringer A 2003 Beyond the visible--imaging the human brain with light. J Cereb Blood Flow Metab 23:1-18.
8. Raichle ME, Mintun MA 2006 Brain work and brain imaging. Annu Rev Neurosci 29:449-476.
9. Ogawa S, Lee TM, Kay AR, Tank DW 1990 Brain magnetic resonance imaging with contrast dependent on blood oxygenation. Proc Natl Acad Sci U S A 87:9868-9872.

10. Peña M, Maki A, Kovacić D, Dehaene-Lambertz G, Koizumi H, Bouquet F, Mehler J 2003 Sounds and silence: an optical topography study of language recognition at birth. Proc Natl Acad Sci U S A 100:11702-11705.

11. Taga G, Asakawa K, Maki A, Konishi Y, Koizumi H 2003 Brain imaging in awake infants by near-infrared optical topography. Proc Natl Acad Sci U S A 100:10722-10727.

12. Liao SM, Gregg NM, White BR, Zeff BW, Bjerkaas KA, Inder TE, Culver JP 2010 Neonatal hemodynamic response to visual cortex activity: high-density near-infrared spectroscopy study. J Biomed Opt 15:026010.

13. Hintz SR, Benaron DA, Siegel AM, Zourabian A, Stevenson DK, Boas DA 2001 Bedside functional imaging of the premature infant brain during passive motor activation. J Perinat Med 29:335-343.

14. Meek JH, Firbank M, Elwell CE, Atkinson J, Braddick O, Wyatt JS 1998 Regional hemodynamic responses to visual stimulation in awake infants. Pediatr Res 43:840-843.

15. Kotilahti K, Nissilä I, Näsi T, Lipiäinen L, Noponen T, Meriläinen P, Huotilainen M, Fellman V 2010 Hemodynamic responses to speech and music in newborn infants. Hum Brain Mapp 31:595-603.

16. Bartocci M, Winberg J, Ruggiero C, Bergqvist LL, Serra G, Lagercrantz H 2000 Activation of olfactory cortex in newborn infants after odor stimulation: a functional near-infrared spectroscopy study. Pediatr Res 48:18-23.

17. Zaramella P, Freato F, Amigoni A, Salvadori S, Marangoni P, Suppiej A, Suppjei A, Schiavo B, Chiandetti L 2001 Brain auditory activation measured by near-infrared spectroscopy (NIRS) in neonates. Pediatr Res 49:213-219.

18. Scholkmann F, Kleiser S, Metz AJ, Zimmermann R, Mata Pavia J, Wolf U, Wolf M 2014 A review on continuous wave functional near-infrared spectroscopy and imaging instrumentation and methodology. Neuroimage 85 Pt 1:6-27.

19. Ferrari M, Quaresima V 2012 A brief review on the history of human functional near-infrared spectroscopy (fNIRS) development and fields of application. Neuroimage 63:921-935.

20. Maki A, Yamashita Y, Ito Y, Watanabe E, Mayanagi Y, Koizumi H 1995 Spatial and temporal analysis of human motor activity using noninvasive NIR topography. Med Phys 22:1997-2005.

21. Franceschini MA, Toronov V, Filiaci M, Gratton E, Fantini S 2000 On-line optical imaging of the human brain with 160-ms temporal resolution. Opt Express 6:49-57.

22. Sato H, Hirabayashi Y, Tsubokura H, Kanai M, Ashida T, Konishi I, Uchida-Ota M, Konishi Y, Maki A 2012 Cerebral hemodynamics in newborn infants exposed to speech sounds: a whole-head optical topography study. Hum Brain Mapp 33:2092-2103.

23. Minagawa-Kawai Y, van der Lely H, Ramus F, Sato Y, Mazuka R, Dupoux E 2011 Optical brain imaging reveals general auditory and language-specific processing in early infant development. Cereb Cortex 21:254-261.

24. Homae F, Watanabe H, Nakano T, Taga G 2011 Large-scale brain networks underlying language acquisition in early infancy. Front Psychol 2:93.

25. Gervain J, Macagno F, Cogoi S, Peña M, Mehler J 2008 The neonate brain detects speech structure. Proc Natl Acad Sci U S A 105:14222-14227.

26. Lloyd-Fox S, Blasi A, Mercure E, Elwell CE, Johnson MH 2011 The emergence of cerebral specialization for the human voice over the first months of life. Soc Neurosci.

27. Grossmann T, Oberecker R, Koch SP, Friederici AD 2010 The developmental origins of voice processing in the human brain. Neuron 65:852-858.

28. Lloyd-Fox S, Blasi A, Volein A, Everdell N, Elwell CE, Johnson MH 2009 Social perception in infancy: a near infrared spectroscopy study. Child Dev 80:986-999.

29. Blasi A, Fox S, Everdell N, Volein A, Tucker L, Csibra G, Gibson AP, Hebden JC, Johnson MH, Elwell CE 2007 Investigation of depth dependent changes in cerebral haemodynamics during face perception in infants. Phys Med Biol 52:6849-6864.

30. Lloyd-Fox S, Blasi A, Elwell CE 2010 Illuminating the developing brain: the past, present and future of functional near infrared spectroscopy. Neurosci Biobehav Rev 34:269-284.

31. Gervain J, Mehler J, Werker JF, Nelson CA, Csibra G, Lloyd-Fox S, Shukla M, Aslin RN 2011 Near-infrared spectroscopy: a report from the McDonnell infant methodology consortium. Dev Cogn Neurosci 1:22-46.

32. Aslin RN, Shukla M, Emberson LL 2015 Hemodynamic correlates of cognition in human infants. Annu Rev Psychol 66:349-379.

33. Vanderwert RE, Nelson CA 2014 The use of near-infrared spectroscopy in the study of typical and atypical development. Neuroimage 85 Pt 1:264-271.

34. Boas DA, Dale AM, Franceschini MA 2004 Diffuse optical imaging of brain activation: approaches to optimizing image sensitivity, resolution, and accuracy. Neuroimage 23 Suppl 1:S275-288.

35. Hoge RD 2012 Calibrated FMRI. Neuroimage 62:930-937.

36. Singh H, Cooper RJ, Wai Lee C, Dempsey L, Edwards A, Brigadoi S, Airantzis D, Everdell N, Michell A, Holder D, Hebden JC, Austin T 2014 Mapping cortical haemodynamics during neonatal seizures using diffuse optical tomography: A case study. Neuroimage Clin 5:256-265.

37. Eggebrecht AT, Ferradal SL, Robichaux-Viehoever A, Hassanpour MS, Dehghani H, Snyder AZ, Hershey T, Culver JP 2014 Mapping distributed brain function and networks with diffuse optical tomography. Nat Photonics 8:448-454.

38. Ferradal SL, Liao SM, Eggebrecht AT, Shimony JS, Inder TE, Culver JP, Smyser CD 2016 Functional Imaging of the Developing Brain at the Bedside Using Diffuse Optical Tomography. Cereb Cortex 26:1558-1568.

39. Arridge SR 2011 Methods in diffuse optical imaging. Philos Trans A Math Phys Eng Sci 369:4558-4576.

40. Hoshi Y, Yamada Y 2016 Overview of diffuse optical tomography and its clinical applications. J Biomed Opt 21:091312.

41. Hielscher AH, Bluestone AY, Abdoulaev GS, Klose AD, Lasker J, Stewart M, Netz U, Beuthan J 2002 Near-infrared diffuse optical tomography. Dis Markers 18:313-337.

42. Chance B, Anday E, Nioka S, Zhou S, Hong L, Worden K, Li C, Murray T, Ovetsky Y, Pidikiti D, Thomas R 1998 A novel method for fast imaging of brain function, non-invasively, with light. Opt Express 2:411-423.

43. Liao SM, Ferradal SL, White BR, Gregg N, Inder TE, Culver JP 2012 High-density diffuse optical tomography of term infant visual cortex in the nursery. J Biomed Opt 17:081414.

44. Biswal BB, Van Kylen J, Hyde JS 1997 Simultaneous assessment of flow and BOLD signals in resting-state functional connectivity maps. NMR Biomed 10:165-170.

45. Doria V, Beckmann CF, Arichi T, Merchant N, Groppo M, Turkheimer FE, Counsell SJ, Murgasova M, Aljabar P, Nunes RG, Larkman DJ, Rees G, Edwards AD 2010 Emergence of resting state networks in the preterm human brain. Proc Natl Acad Sci U S A 107:20015-20020.

46. Smyser CD, Inder TE, Shimony JS, Hill JE, Degnan AJ, Snyder AZ, Neil JJ 2010 Longitudinal analysis of neural network development in preterm infants. Cereb Cortex 20:2852-2862.

47. Fransson P, Skiöld B, Engström M, Hallberg B, Mosskin M, Aden U, Lagercrantz H, Blennow M 2009 Spontaneous brain activity in the newborn brain during natural sleep--an fMRI study in infants born at full term. Pediatr Res 66:301-305.

48. Fransson P, Skiöld B, Horsch S, Nordell A, Blennow M, Lagercrantz H, Aden U 2007 Resting-state networks in the infant brain. Proc Natl Acad Sci U S A 104:15531-15536.

49. White BR, Liao SM, Ferradal SL, Inder TE, Culver JP 2012 Bedside optical imaging of occipital resting-state functional connectivity in neonates. Neuroimage 59:2529-2538.

50. Lawn J, Shibuya K, Stein C 2005 No cry at birth: global estimates of intrapartum stillbirths and intrapartum-related neonatal deaths. Bull World Health Organ 83:409-417.

51. Volpe JJ 2001 Perinatal brain injury: from pathogenesis to neuroprotection. Ment Retard Dev Disabil Res Rev 7:56-64.

52. Cooper RJ, Hebden JC, O'Reilly H, Mitra S, Michell AW, Everdell NL, Gibson AP, Austin T 2011 Transient haemodynamic events in neurologically compromised infants: a simultaneous EEG and diffuse optical imaging study. Neuroimage 55:1610-1616.

53. Hellstrom-Westas L, Rosen I 2010 Electroencephalography and amplitude-integrated EEG. In Lagercrantz H (ed) The Newborn Brain: Neuroscience and Clinical Applications. Cambridge University Press, pp 211-228.

54. Lewis LD, Ching S, Weiner VS, Peterfreund RA, Eskandar EN, Cash SS, Brown EN, Purdon PL 2013 Local cortical dynamics of burst suppression in the anaesthetized brain. Brain 136:2727-2737.

55. Chalia M, Lee CW, Dempsey LA, Edwards AD, Singh H, Michell AW, Everdell NL, Hill RW, Hebden JC, Austin T, Cooper RJ 2016 Hemodynamic response to burst-suppressed and discontinuous electroencephalography activity in infants with hypoxic ischemic encephalopathy. Neurophotonics 3:10.

56. Torricelli A, Contini D, Pifferi A, Caffini M, Re R, Zucchelli L, Spinelli L 2014 Time domain functional NIRS imaging for human brain mapping. Neuroimage 85 Pt 1:28-50.

57. Hebden JC, Gibson A, Yusof RM, Everdell N, Hillman EM, Delpy DT, Arridge SR, Austin T, Meek JH, Wyatt JS 2002 Three-dimensional optical tomography of the premature infant brain. Phys Med Biol 47:4155-4166.

58. Austin T, Gibson AP, Branco G, Yusof RM, Arridge SR, Meek JH, Wyatt JS, Delpy DT, Hebden JC 2006 Three dimensional optical imaging of blood volume and oxygenation in the neonatal brain. Neuroimage 31:1426-1433.

59. Hintz SR, Benaron DA, van Houten JP, Duckworth JL, Liu FW, Spilman SD, Stevenson DK, Cheong WF 1998 Stationary headband for clinical time-of-flight optical imaging at the bedside. Photochem Photobiol 68:361-369.

60. Hintz SR, Cheong WF, van Houten JP, Stevenson DK, Benaron DA 1999 Bedside imaging of intracranial hemorrhage in the neonate using light: comparison with ultrasound, computed tomography, and magnetic resonance imaging. Pediatr Res 45:54-59.

61. Hebden JC, Gibson A, Austin T, Yusof RM, Everdell N, Delpy DT, Arridge SR, Meek JH, Wyatt JS 2004 Imaging changes in blood volume and oxygenation in the

newborn infant brain using three-dimensional optical tomography. Phys Med Biol 49:1117-1130.

62. Gibson AP, Austin T, Everdell NL, Schweiger M, Arridge SR, Meek JH, Wyatt JS, Delpy DT, Hebden JC 2006 Three-dimensional whole-head optical tomography of passive motor evoked responses in the neonate. Neuroimage 30:521-528.

63. Brigadoi S, Ceccherini L, Cutini S, Scarpa F, Scatturin P, Selb J, Gagnon L, Boas DA, Cooper RJ 2013 Motion artifacts in functional near-infrared spectroscopy: A comparison of motion correction techniques applied to real cognitive data. Neuroimage.

64. Barker JW, Rosso AL, Sparto PJ, Huppert TJ 2016 Correction of motion artifacts and serial correlations for real-time functional near-infrared spectroscopy. Neurophotonics 3:031410.

65. Gu Y, Han J, Liang Z, Yan J, Li Z, Li X 2016 Empirical mode decomposition-based motion artifact correction method for functional near-infrared spectroscopy. J Biomed Opt 21:15002.

66. Gagnon L, Perdue K, Greve DN, Goldenholz D, Kaskhedikar G, Boas DA 2011 Improved recovery of the hemodynamic response in diffuse optical imaging using short optode separations and state-space modeling. Neuroimage 56:1362-1371.

67. Saager R, Berger A 2008 Measurement of layer-like hemodynamic trends in scalp and cortex: implications for physiological baseline suppression in functional near-infrared spectroscopy. J Biomed Opt 13:034017.

68. Gregg NM, White BR, Zeff BW, Berger AJ, Culver JP 2010 Brain specificity of diffuse optical imaging: improvements from superficial signal regression and tomography. Front Neuroenergetics 2.

69. Markham J, White BR, Zeff BW, Culver JP 2009 Blind identification of evoked human brain activity with independent component analysis of optical data. Hum Brain Mapp 30:2382-2392.

70. Zhang H, Zhang YJ, Lu CM, Ma SY, Zang YF, Zhu CZ 2010 Functional connectivity as revealed by independent component analysis of resting-state fNIRS measurements. Neuroimage 51:1150-1161.

71. Franceschini MA, Joseph DK, Huppert TJ, Diamond SG, Boas DA 2006 Diffuse optical imaging of the whole head. J Biomed Opt 11:054007.

72. Zhang Y, Brooks DH, Franceschini MA, Boas DA 2005 Eigenvector-based spatial filtering for reduction of physiological interference in diffuse optical imaging. J Biomed Opt 10:11014.

73. Virtanen J, Noponen T, Merilainen P 2009 Comparison of principal and independent component analysis in removing extracerebral interference from near-infrared spectroscopy signals. J Biomed Opt 14:054032.

74. Brigadoi S, Aljabar P, Kuklisova-Murgasova M, Arridge SR, Cooper RJ 2014 A 4D neonatal head model for diffuse optical imaging of pre-term to term infants. Neuroimage 100:385-394.

75. Ferradal SL, Eggebrecht AT, Hassanpour M, Snyder AZ, Culver JP 2014 Atlas-based head modeling and spatial normalization for high-density diffuse optical tomography: in vivo validation against fMRI. Neuroimage 85 Pt 1:117-126.

76. Cooper RJ, Caffini M, Dubb J, Fang Q, Custo A, Tsuzuki D, Fischl B, Wells W, Dan I, Boas DA 2012 Validating atlas-guided DOT: a comparison of diffuse optical tomography informed by atlas and subject-specific anatomies. Neuroimage 62:1999-2006.

77. Tak S, Ye JC 2014 Statistical analysis of fNIRS data: a comprehensive review. Neuroimage 85 Pt 1:72-91.

78. Friston KJ, Holmes AP, Poline JB, Grasby PJ, Williams SC, Frackowiak RS, Turner R 1995 Analysis of fMRI time-series revisited. Neuroimage 2:45-53.

79. Ye JC, Tak S, Jang KE, Jung J, Jang J 2009 NIRS-SPM: statistical parametric mapping for near-infrared spectroscopy. Neuroimage 44:428-447.

80. Hassanpour MS, White BR, Eggebrecht AT, Ferradal SL, Snyder AZ, Culver JP 2014 Statistical analysis of high density diffuse optical tomography. Neuroimage 85 Pt 1:104-116.

81. Huppert TJ 2016 Commentary on the statistical properties of noise and its implication on general linear models in functional near-infrared spectroscopy. Neurophotonics 3:010401.

82. Chitnis D, Airantzis D, Highton D, Williams R, Phan P, Giagka V, Powell S, Cooper RJ, Tachtsidis I, Smith M, Elwell CE, Hebden JC, Everdell N 2016 Towards a wearable near infrared spectroscopic probe for monitoring concentrations of multiple chromophores in biological tissue in vivo. Rev Sci Instrum 87:065112.

83. Amal Kassab and Jr, me Le Lan and Phetsamone Vannasing and Mohamad S 2015 Functional near-infrared spectroscopy caps for brain activity monitoring: a review. Appl. Opt. 54:576--586.

References for Figures

Figure 2b: Hillman EM. Optical brain imaging in vivo: techniques and applications from animal to man. J Biomed Opt 2007;12:051402.

Figure 3a: Singh H, Cooper RJ, Wai Lee C, et al. Mapping cortical haemodynamics during neonatal seizures using diffuse optical tomography: A case study. Neuroimage Clin 2014;5:256-65.

Figure 3b: Singh H, Cooper RJ, Wai Lee C, et al. Mapping cortical haemodynamics during neonatal seizures using diffuse optical tomography: A case study. Neuroimage Clin 2014;5:256-65.

Figure 3e: Brigadoi S, Aljabar P, Kuklisova-Murgasova M, Arridge SR, Cooper RJ. A 4D neonatal head model for diffuse optical imaging of pre-term to term infants. Neuroimage 2014;100:385-94.

Figure 3f: Brigadoi S, Aljabar P, Kuklisova-Murgasova M, Arridge SR, Cooper RJ. A 4D neonatal head model for diffuse optical imaging of pre-term to term infants. Neuroimage 2014;100:385-94.

Figure 4: Ferradal SL, Liao SM, Eggebrecht AT, et al. Functional Imaging of the Developing Brain at the Bedside Using Diffuse Optical Tomography. Cereb Cortex 2016;26:1558-68.

Figure 5: Cooper RJ, Hebden JC, O'Reilly H, et al. Transient haemodynamic events in neurologically compromised infants: a simultaneous EEG and diffuse optical imaging study. Neuroimage 2011;55:1610-6.

Figure 6: Singh H, Cooper RJ, Wai Lee C, et al. Mapping cortical haemodynamics during neonatal seizures using diffuse optical tomography: A case study. Neuroimage Clin 2014;5:256-65.

Figure 7b: Austin T, Gibson AP, Branco G, et al. Three dimensional optical imaging of blood volume and oxygenation in the neonatal brain. Neuroimage 2006;31:1426-33.

Figure 7c: Austin T, Gibson AP, Branco G, et al. Three dimensional optical imaging of blood volume and oxygenation in the neonatal brain. Neuroimage 2006;31:1426-33.

Figure Legends

Figure 1

A decision tree that provides a definition of the different forms of diffuse optical monitoring. While nomenclature varies across the field, these are the definitions preferred by the authors.

Figure 2

(a) The absorption properties of oxy- (red line), deoxyhemoglobin (green line) and water (blue line) in biological tissue. In the optical window (shaded in blue) between 700 and 900 nm, light is relatively transparent as the absorption by water molecules is relatively low compared to oxy- and deoxyhemoglobin.

(b) The path of near-infrared light from an optical source follows a banana-shape as it travels in cerebral tissue before the transmitted light is measured at the detector.

(c) The UCL Optical Imaging System (Gowerlabs, London). This is a continuous wave device that samples at 10Hz and provides 16 optical sources and 16 detectors.

(d) An example of headgear design used in infant studies of whole-head diffuse optical tomography.

Figure 3

Diffuse Optical Tomography Image Reconstruction

(a) A photo of the headgear used in infant whole-head diffuse optical tomography scanning.

(b) A schematic of the locations of sources (red dots) and detectors (blue dots) of the headgear in (a). The black lines represent source-detector channels.

(c) During scanning, raw light intensity data is converted to changes in optical density and these are assigned to the location of the source-detector channels of the headgear array.

(d) An anatomical MRI is required to provide structural information for image reconstruction. This can either be the infant's own MRI or an age-matched atlas may be used.

(e) The anatomical MRI image is segmented to identify the different tissue types (such as scalp, cerebrospinal fluid, gray matter, white matter) as these will have different optical properties.

(f) A mathematical model of how light will travel through brain tissue is derived. This will define how light intensity measured at a detector will change given localized changes in oxy- and deoxyhemoglobin.

(g) A sensitivity matrix describing how the changes in light intensity at each channel location (from b) relates to the changes in oxy- and deoxyhemoglobin concentration (the final desired image) can be calculated using the model of light propagation in tissue from (f).

(h) The desired image is reconstructed by combining the properties of the sensitivity matrix (g) with the channel data (c).

Figure 4

Resting state functional connectivity maps from a single healthy term infant. The first column indicates the regions of interest selected for seed-based analysis of the visual (vis), middle temporal (MT) and primary auditory (A1) networks. The second column displays the correlation maps (i.e. networks) for each region of interest from functional connectivity diffuse optical tomography (fcDOT). The oxyhemoglobin signal (ΔHbO_2) from DOT is overlaid on the subject-specific anatomical MRI image. The third column displays the correlation maps for each region of interest using the blood oxygen level dependent (BOLD) signal in fMRI.

Figure 5

DOT images reconstructed from a neurologically compromised infant for a single hemodynamic event. The series of images are reconstructed at a depth of 9-12 mm from the left lateral surface at 95 s preceding, to 95 s after the event. Red indicates an increase, and blue a decrease in the concentration of oxyhemoglobin.

Figure 6

DOT images reconstructed in an infant with severe hypoxic ischemic encephalopathy. The upper graph illustrates the oxy- (HbO, red line), deoxy- (HbR, blue line) and total hemoglobin (HbT, green line) changes for a seizure event identified by electroencephalography (EEG), which was recorded simultaneously. The numbered images below represent the cortical changes in 3 different views (dorsal, left and right lateral) seen during the different time points of the seizure event as depicted in the graph. Red indicates an increase, and blue a decrease in the total hemoglobin (HbT) concentration in the DOT images.

Figure 7

(a) A photo of the UCL time-domain DOT system (MONSTIR II) in the Rosie Hospital, Cambridge, UK.

(b) A cranial ultrasound of a preterm infant revealing a left sided intraventricular hemorrhage and hemorrhagic parenchymal infarct.

(c) A 3D-DOT image taken at a coronal section of the same preterm infant showing regional blood volume (left) and oxygen saturation (right). There is an increase in hemoglobin concentration and decrease in oxygen saturation in the area corresponding to the hemorrhage and infarct.

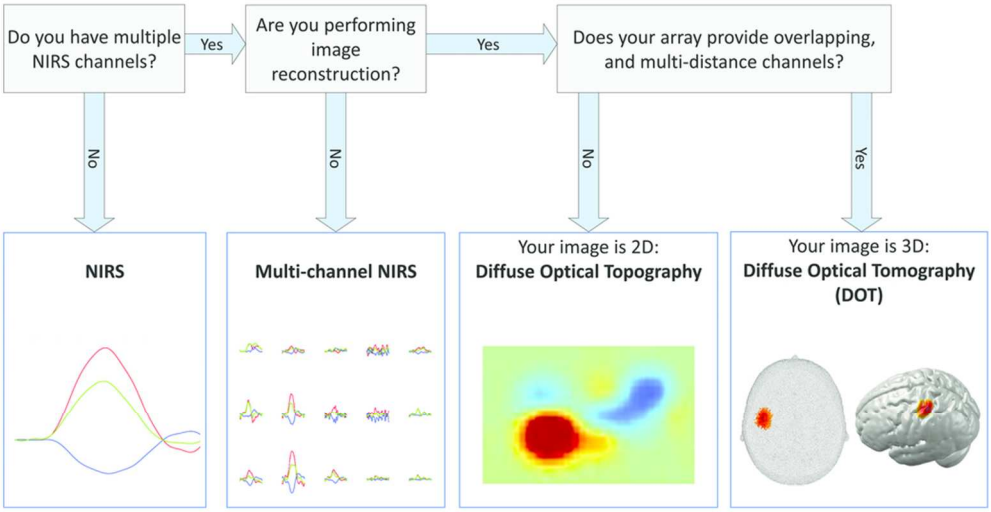

A decision tree that provides a definition of the different forms of diffuse optical monitoring. While nomenclature varies across the field, these are the definitions preferred by the authors.

88x46mm (300 x 300 DPI)

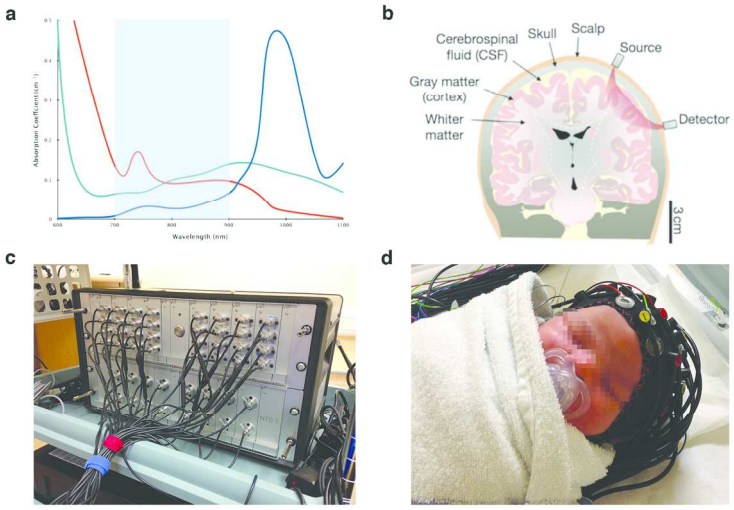

(a) The absorption properties of oxy- (red line), deoxyhemoglobin (green line) and water (blue line) in biological tissue. In the optical window (shaded in blue) between 700 and 900 nm, light is relatively transparent as the absorption by water molecules is relatively low compared to oxy- and deoxyhemoglobin.
(b) The path of near-infrared light from an optical source follows a banana-shape as it travels in cerebral tissue before the transmitted light is measured at the detector.
(c) The UCL Optical Imaging System (Gowerlabs, London). This is a continuous wave device that samples at 10Hz and provides 16 optical sources and 16 detectors.
(d) An example of headgear design used in infant studies of whole-head diffuse optical tomography.

180x96mm (300 x 300 DPI)

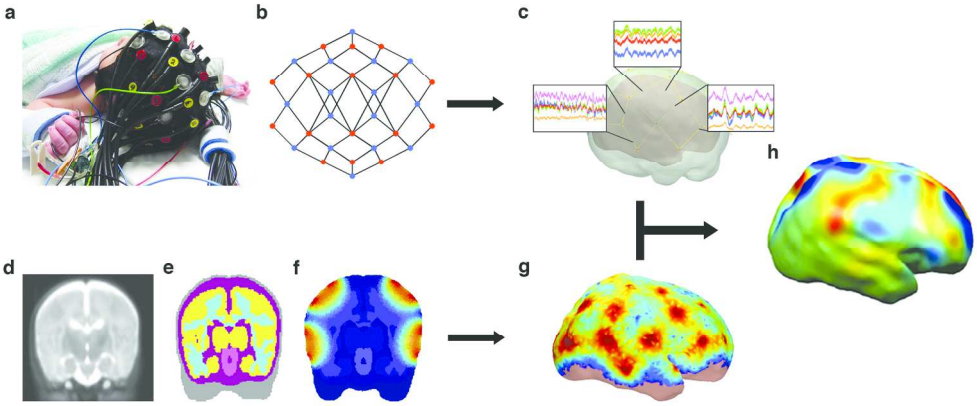

Diffuse Optical Tomography Image Reconstruction: (a) A photo of the headgear used in infant whole-head diffuse optical tomography scanning. (b) A schematic of the locations of sources (red dots) and detectors (blue dots) of the headgear in (a). The black lines represent source-detector channels. (c) During scanning, raw light intensity data is converted to changes in optical density and these are assigned to the location of the source-detector channels of the headgear array. (d) An anatomical MRI is required to provide structural information for image reconstruction. This can either be the infant's own MRI or an age-matched atlas may be used. (e) The anatomical MRI image is segmented to identify the different tissue types (such as scalp, cerebrospinal fluid, gray matter, white matter) as these will have different optical properties. (f) A mathematical model of how light will travel through brain tissue is derived. This will define how light intensity measured at a detector will change given localized changes in oxy- and deoxyhemoglobin. (g) A sensitivity matrix describing how the changes in light intensity at each channel location (from b) relates to the changes in oxy- and deoxyhemoglobin concentration (the final desired image) can be calculated using the model of light propagation in tissue from (f). (h) The desired image is reconstructed by combining the properties of the sensitivity matrix (g) with the channel data (c).

180x77mm (300 x 300 DPI)

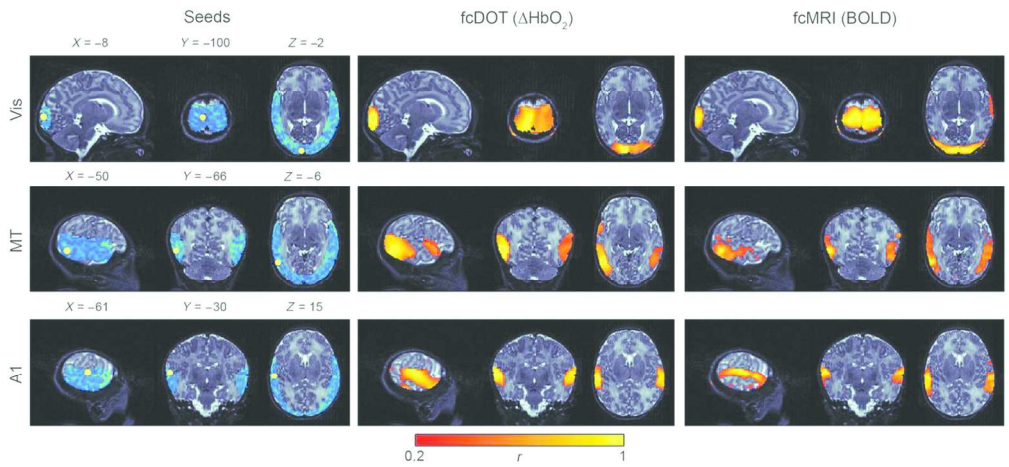

Resting state functional connectivity maps from a single healthy term infant. The first column indicates the regions of interest selected for seed-based analysis of the visual (vis), middle temporal (MT) and primary auditory (A1) networks. The second column displays the correlation maps (i.e. networks) for each region of interest from functional connectivity diffuse optical tomography (fcDOT). The oxyhemoglobin signal (ΔHbO2) from DOT is overlaid on the subject-specific anatomical MRI image. The third column displays the correlation maps for each region of interest using the blood oxygen level dependent (BOLD) signal in fMRI.

180x85mm (300 x 300 DPI)

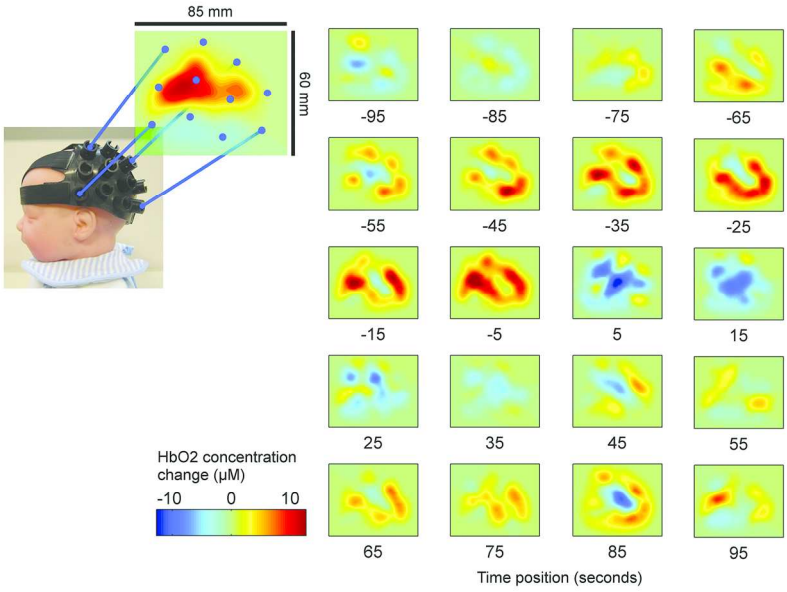

DOT images reconstructed from a neurologically compromised infant for a single hemodynamic event. The series of images are reconstructed at a depth of 9-12 mm from the left lateral surface at 95 s preceding, to 95 s after the event. Red indicates an increase, and blue a decrease in the concentration of oxyhemoglobin.

180x107mm (300 x 300 DPI)

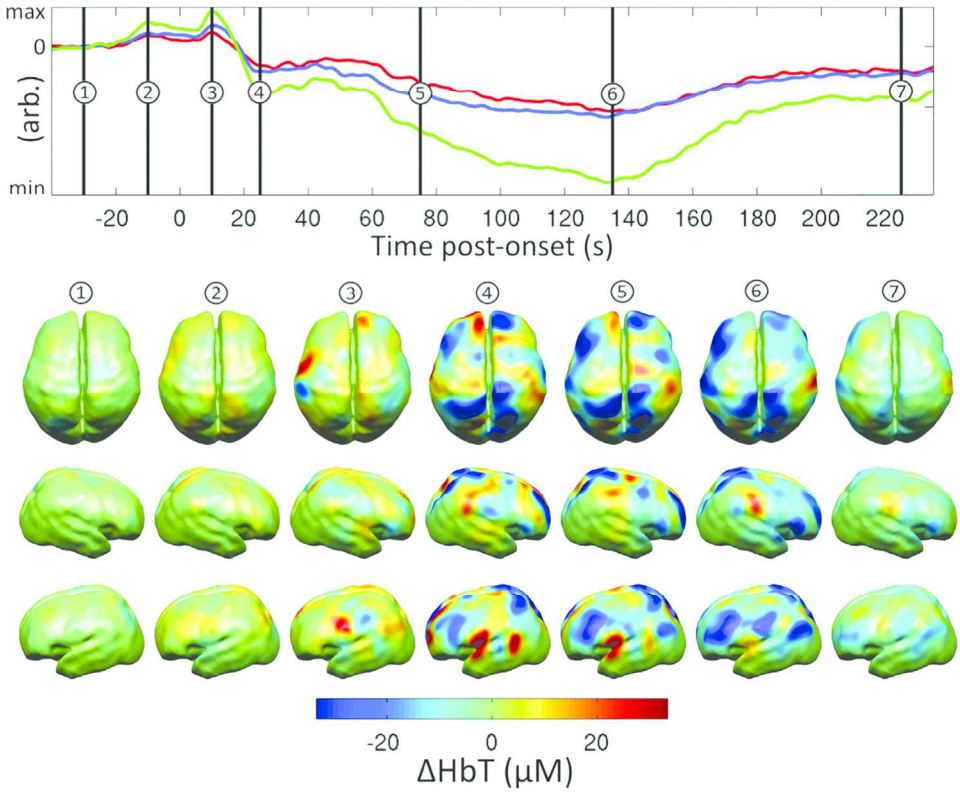

DOT images reconstructed in an infant with severe hypoxic ischemic encephalopathy. The upper graph illustrates the oxy- (HbO, red line), deoxy- (HbR, blue line) and total hemoglobin (HbT, green line) changes for a seizure event identified by electroencephalography (EEG), which was recorded simultaneously. The numbered images below represent the cortical changes in 3 different views (dorsal, left and right lateral) seen during the different time points of the seizure event as depicted in the graph. Red indicates an increase, and blue a decrease in the total hemoglobin (HbT) concentration in the DOT images.

180x145mm (300 x 300 DPI)

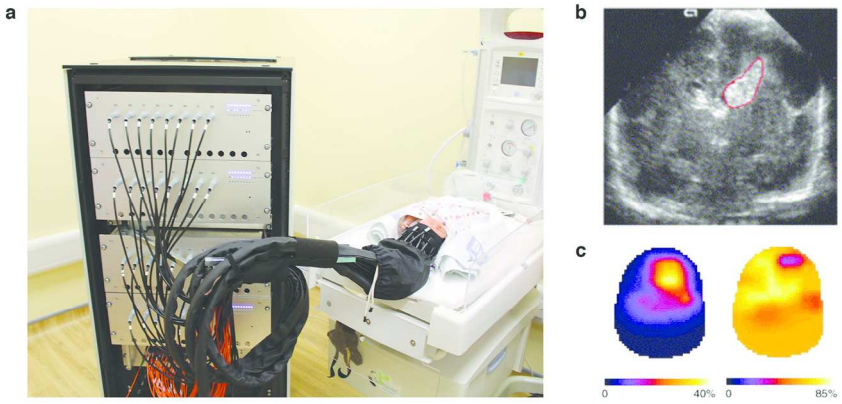

(a) A photo of the UCL time-domain DOT system (MONSTIR II) in the Rosie Hospital, Cambridge, UK. (b) A cranial ultrasound of a preterm infant revealing a left sided intraventricular hemorrhage and hemorrhagic parenchymal infarct. (c) A 3D-DOT image taken at a coronal section of the same preterm infant showing regional blood volume (left) and oxygen saturation (right). There is an increase in hemoglobin concentration and decrease in oxygen saturation in the area corresponding to the hemorrhage and infarct.

180x76mm (300 x 300 DPI)